Knowledge Discovery Pipeline for the Diagnosis of Tuberculosis

By

Saira Kiran

(NUST00000364955-MSBI-Fall21)

(MS Bioinformatics)

Supervised by:

Dr. Ishrat Jabeen

School of Interdisciplinary Engineering & Sciences

National University of Sciences & Technology

Islamabad, Pakistan

August 2023

Annex A to NUST Letter No. 0972/102/Exams/Thesis-Cert dated 10 August 2023.

16/8/23

THESIS ACCEPTANCE CERTIFICATE

Certified that final copy of MS/MPhil thesis written by Mr/Ms Saira Kiran Registration No. 00000364955 of SINES has been vetted by undersigned, found complete in all aspects as per NUST Statutes/Regulations, is free of plagiarism, errors, and mistakes and is accepted as partial fulfillment for award of MS/MPhil degree. It is further certified that necessary amendments as pointed out by GEC members of the scholar have also been incorporated in the said thesis.

Signature with stamp: _____

Name of Supervisor: Dr Ishrat Jabeen

DR. ISHRAT JABEEN
Professor
School of Interdisciplinary Engineering & Sciences
NUST Sector H-12 Islamabad

Date: 10/08/2023

Signature of HoD with stamp: _____

Associate Professor
SINES - NUST, Sector H-12
Islamabad

Date: 16 AUG 2023

Countersign by

Signature (Dean/Principal): _____

Dr. Hammad M. Cheema
Principal & Dean
SINES - NUST, Sector H-12
Islamabad

Date: 28/08/2023

Certificate of Originality

I hereby certify that the research work presented in this thesis is entirely my own and has been conducted independently. All the references and sources utilized in preparing this thesis have been duly acknowledged. I further declare that this thesis has not been previously submitted for any other degree or examination.

Saira Kiran

(NUST00000364955-MSBI-Fall21)

Dedication

I dedicated this thesis to my parents, Muhammad Ali, Yasmeen and my grandmother, Shameem Akhtar whose unconditional support, encouragement, and sacrifices have been the foundation of my achievements.

ACKNOWLEDGMENT

I am deeply grateful to Almighty Allah for providing me with this incredible opportunity to achieve my academic goals. I sincerely appreciate all my instructors who imparted knowledge and guidance throughout my pursuit of an MS degree. In particular, I am immensely grateful to my research supervisor *Professor Dr. Ishrat Jabeen*, for her valuable guidance and unwavering support throughout my research project. I am also thankful to my research guidance committee member, *Dr Muhammad Tariq Saeed* and *Dr Ammar Mushtaq*, for their insightful comments and encouragement. I would also like to acknowledge skilled engineers and assistants at the SINES labs for their technical support.

My parents, Muhammad Ali and Yasmeen, whose emotional and financial support helped me achieve my goals. Their belief in my abilities and constant support has been vital in helping me achieve this milestone. I also acknowledge my grandmother, Shameem Akhtar and younger sisters, Taiba Ali, and Kubra Ali.

Moreover, I would like to express my deep appreciation to *Mr. Taimoor Khan* and *Mr Raja Mehtab* for their invaluable assistance in obtaining the hospital's necessary data collection permissions. I am deeply thankful for their efforts and contributions to the success of my research project. I am also very thankful to the Medical Superintendent of Syed Muhammad Hussain TB Sanatorium, Samli, Pakistan, *Dr Qaiser Mehmood Abbasi*, for permitting me to collect the data of patients. I would extend my gratitude to Mr Ahsan Ahmad, the facilitator of DOTS (Directly Observed Treatment) and head of the TB dispensary at the hospital, for his assistance in the daily data collection. I would also like to thank *Dr Athar* and *Dr Kinza* for supporting me throughout my journey of data collection.

Furthermore, I would like to thank all my colleagues for fostering a positive learning environment in the lab.

Saira Kiran

Table of Contents

LIST OF FIGURES

LIST OF TABLES

LIST OF ABBREVIATIONS

CNN	Convolutional Neural Network
DL	Deep Learning
ML	Machine Learning
TB	Tuberculosis
COVID-19	Coronavirus Disease 2019
CXR	Chest X-Ray
AI	Artificial Intelligence
ROI	Region of Interest
ROC	Receiver Operating Characteristics
AUC	The area under the Curve
RGB	Red Green Blue
TP	True Positives
TN	True Negatives
FP	False Positives
FN	False Negatives
CM	Confusion Matrix
VGG	Visual Geometry Group
ResNet	Residual Network
Densenet	Densely Connected Convolutional Networks

Abstract

Accurate and early tuberculosis (TB) diagnosis is very important for efficient disease management. Chest X-rays are widely used for the TB diagnosis that infects a high number of people worldwide. The manual examination of chest X-rays is challenging and it is limited by the need for expert doctors. Moreover, TB chest X-ray is often misclassified to some other disease conditions of similar patterns such as COVID-19 and pneumonia. Chest X-ray misclassification can potentially lead to delayed treatment and disease spread. In recent years, deep-learning approaches have shown great promise in image analysis, particularly in medical image analysis. This study aims to focus on the automated detection of TB in chest X-rays using deep learning approaches. A comprehensive dataset consisting of 2500 TB, 2517 normal, and 2522 COVID-19 chest X-ray images was collected from different local hospitals in Pakistan and preprocessed. A convolutional neural network (CNN) has been employed for classification, and the performance of the CNN has been compared with different pre-trained deep learning models, including VGG-16, ResNet-50, InceptionV3, and DenseNet-121. Accuracy, precision, recall, and F1-Score were also calculated to evaluate the model performances. Out of all the models, CNN achieved a higher accuracy of 97.67%. The results obtained indicate the CNN model's effectiveness in accurately classifying TB from chest X-rays. The trained CNN model was deployed into a user-friendly web application for real-time diagnosis. This study contributes to the field of image analysis by highlighting deep learning's potential in TB diagnosis. For radiologists and other medical experts, the developed CNN is a valuable tool assisting them in TB diagnosis more accurately and efficiently.

CHAPTER 1
INTRODUCTION

1. Introduction

1.1 Tuberculosis

Tuberculosis (TB) is highly infectious and life-threatening disease. It is caused by a slow-growing bacteria named Bacillus Mycobacterium tuberculosis that grows in blood and oxygen-rich organs of the body such as the lungs. The bacteria mainly affects the lungs in 80% of cases, but it can also affect other body parts [1]. According to the world health organization, around 10 million people annually become infected with tuberculosis, and a total of 1.5 million people die from it [2]. In 2021, an estimated 10.6 million people fall ill with tuberculosis and 1.6 million people died from tuberculosis globally [3]. TB is one of the top ten major causes of death worldwide, and it is the second infectious killer after COVID-19 [4]. More than 80% of deaths and cases due to tuberculosis are in low-resource countries [5]. The mycobacterium tuberculosis bacteria that cause TB can move from person to person through the air. TB bacteria can enter the air when a person with lung TB disease coughs, sneezes, spits, sings, or even talks. When someone breathes in TB bacteria, the bacteria may congregate in the lungs and start to develop. [6]. However, TB cannot be spread by shaking hands, sharing clothes, or using shared utensils. People need to inhale only a few of these TB bacteria to become infected with TB [7]. People who are in close contact with TB-infected individuals are at high risk of getting TB disease. To prevent the spread of the disease, people who are infected with TB should keep their mouth and nose covered while coughing or sneezing, refrain from going to work or school until they are no longer contagious, and complete their treatment as prescribed. Moreover, individuals who are susceptible to TB infection, such as healthcare workers and HIV-positive people, should undergo routine TB testing. The symptoms of TB disease might differ depending on the part of the body that is affected, but the most common symptoms are a persistent cough, night sweats, lack of appetite, weight loss, chest pain, blood in cough, fever, and fatigue. Generally, it is very challenging to diagnose TB disease because its symptoms closely resemble those of other pulmonary diseases such as COVID-19, pneumonia, etc. [8]. However, TB is treatable and curable with a combination of antibiotics, but the treatment can be lengthy, lasting between six and nine months and can be deadly if left untreated [9]. TB is a serious public health issue in low-resource countries and a leading cause of death. Although TB is present worldwide, most TB patients reside in low- and middle-income countries [10]. Eight countries; Bangladesh,

Pakistan, China, India, Indonesia, Nigeria, Philippines, and South Africa account for about 50 % of all TB cases [11]. In many low-resource countries, factors such as poverty, malnutrition, overcrowding, and limited access to healthcare facilities contribute to the high burden of TB. According to the World Health Organization (WHO), in 2020, an estimated 10 million people developed TB globally, with 85% of new cases occurring in low and middle-income countries [12].

1.2 Types of Tuberculosis

Latent tuberculosis and active tuberculosis are the two main types of tuberculosis (TB). Based on the location of the infection, there are several types of TB.

1.2.1 Latent TB

Latent TB is when Mycobacterium tuberculosis bacteria infect and live in the body without any symptoms [13]. Latent TB patients are not contagious and are unable to transmit the bacteria to others. In latent TB conditions, the infected person's immune system may be able to control the infection and prevent it from spreading. Occasionally, the bacteria may continue to exist in the body while being dormant, which means they are not growing or harming the person. Many people with latent TB infection never develop active TB for the majority of their lives. However, if the bacteria become active and begin to multiply, latent TB in some people can turn into active TB. This may occur if a person's immune system is weakened as a result of illness or medication, or exposure to someone with active TB disease. Chest X-rays are not frequently used to diagnose latent TB since latent TB does not show any symptoms and does not harm the lungs in the same way as active TB. Typically, a skin test or blood test is used to identify the presence of TB antibodies or cells in the immune system. If a person tests positive for latent TB, taking antibodies may be suggested to prevent the latent TB condition from turning into active TB disease. Antibodies kill the bacteria and prevent the development of active TB disease. However, to guarantee that the infection is completely treated, it is crucial to finish the course of antibodies. If a person with a weakened immune system does not complete the course of antibodies or left TB untreated then the latent TB can develop into active TB, leading to serious illness and even being fatal in some cases. Therefore, it is very important to get tested for TB if you have recently come into contact with someone who has active TB disease or if you are at high risk of infection [14] [15].

1.2.2 Active TB

Active TB commonly known as TB disease in which the mycobacterium tuberculosis bacteria rapidly grow and multiply. Active TB is the most prevalent type of TB [16] exhibiting many symptoms including chest pain, weight loss, night sweats, coughing up blood, or sputum, weakness, loss of appetite, fever, and persistent severe cough lasting three weeks or longer. People who have active TB may transmit the TB bacteria to others [17] [18]. Pulmonary TB and Extra pulmonary TB are two different conditions of active TB. Active tuberculosis can occur in the lungs (pulmonary TB) or other parts of the body (extra-pulmonary TB) [19]. In Active TB disease, when a person breathes, TB bacteria can enter the lungs and begin to grow. Tubercles, which are small, spherical nodules, may develop as a result of bacterial multiplication. As the bacteria continue to multiply, the tubercles may enlarge and converge, forming greater areas of infection in the lungs. This may harm the lung tissues and result in the development of holes or cavities in the lungs. In addition to the lungs, active TB disease can also expand to the lymph nodes, bones, joints, meninges, and the genitourinary system [20]. Moreover, active TB can also affect the skin, eyes, and gastrointestinal tract. A medical history, physical examination, and laboratory testing, such as sputum cultures, chest X-rays, and other procedures to detect the presence of TB bacteria, are frequently used to diagnose active TB. Chest X-rays are most commonly and widely used to diagnose active pulmonary TB disease, as active TB causes changes in the lungs that can be seen on a chest X-ray. Active TB disease can spread from person to person through the air when an infected individual coughs or sneezes and become contagious. Therefore, it is very important to take preventative steps to stop the spread of TB disease, such as maintaining excellent cleanliness, wearing a mask, and avoiding close contact with those who are suffering from an active TB disease. Depending on the location and severity of the bacteria infection, there are various forms of TB within these two pulmonary and extra-pulmonary [21].

1.2.3 Pulmonary TB

Pulmonary TB, which affects the lungs, is the most common form of TB. It is responsible for 85% of all TB cases worldwide [22]. Pulmonary TB may be symptomatic or asymptomatic pulmonary TB. Asymptomatic pulmonary TB refers to the infection of TB bacteria in a person who shows no symptoms of the disease. This type of TB is frequently diagnosed through routine examination or contact tracing. Symptomatic pulmonary TB is characterized by chest

pain, a persistent cough that lasts three weeks or longer, coughing up blood and mucus, and breathing issues in addition to regular TB symptoms [23]. Pulmonary TB can be identified using a variety of TB diagnostic tests, such as Chest X-rays, sputum smear microscopy, and molecular diagnostic assays like GeneXpert. Neglecting pulmonary TB can be fatal because it can cause serious lung damage and be life-threatening. Additionally, it might cause extrapulmonary TB by transferring the infection to different body areas. People should cover their mouths when they cough or sneeze, increase ventilation in their homes and places of employment, and have access to TB testing, diagnosis, and treatment to prevent pulmonary TB [24].

1.2.4 Drug-resistant TB

Drug-resistant TB occurs when the Mycobacterium tuberculosis bacteria develop resistance to one or more of the antibiotics used to treat the infection. According to the world health organization, the majority of drug-resistant tuberculosis cases, with multidrug-resistant tuberculosis (MDR-TB) being the most prevalent kind of drug-resistant tuberculosis, account for about 5% of all TB cases [25]. Multidrug-resistant TB (MDR-TB) and extensively drug-resistant TB (XDR-TB) are the two primary kinds of drug-resistant TB, depending on the type and degree of resistance. At least two of the most powerful first-line TB medications, isoniazid and rifampicin, are ineffective against MDR-TB. [26]. XDR-TB is more deadly since it is resistant to at least four of the most effective TB drugs, including both first-line and second-line drugs [27]. Drug-resistant tuberculosis is a growing global health concern, particularly in areas where the prevalence of the disease is high, such as sub-Saharan Africa and Asia [28] [29]. It is usually caused by incorrect or incomplete treatment of TB, which enables the bacteria to adapt and build up resistance to the medications used to treat it. Drug-resistant TB is more challenging to treat and may require longer more complex treatment. In contrast to standard TB treatment, it requires a combination of different antibiotics for a longer period. The course of treatment may last up to two years and may come with more severe side effects than standard TB treatment. To stop the spread of drug-resistant TB, prevention is essential. This includes ensuring that all TB patients receive the proper treatment and are monitored for drug resistance, as well as improving infection control measures to stop the spread of TB in healthcare settings and the general public.

While pulmonary tuberculosis (TB) is the most common form of TB, several rare types of tuberculosis can affect different parts of the body. Some examples of rare types of TB include Miliary TB, skeletal TB, genitourinary TB, etc.

1.2.5 Extra-pulmonary TB

Extra-pulmonary TB occurs when bacteria infect parts of the body other than the lungs such as the kidneys, bones, lymph nodes, joints, and central nervous system. Extra-pulmonary TB is rare. Approximately it accounts for about 15%-20% of all TB cases [30] [31]. The site of the infection affects the extra-pulmonary TB symptoms. For instance, TB which affects the bones and joints can result in pain, discomfort, and decreased movement, whereas TB which affects the brain can result in headaches, confusion, and seizures. Some of the common locations for extra-pulmonary TB are the bones, lymph nodes, joints meninges, and genitourinary system (including the kidneys, bladder, and reproductive organs). Extra-pulmonary TB can also affect the eyes, skin, and gastrointestinal tract. Extra-pulmonary tuberculosis is often diagnosed using a combination of laboratory tests such as medical imaging (x-rays and CT scans etc.), physical examination, and medical history. Extra-pulmonary tuberculosis is rare and less contagious than pulmonary tuberculosis, which means that it is less likely to spread from person to person. However, it is still crucial to take preventative measures to stop the spread of TB, such as maintaining excellent hygiene and avoiding close contact with those who are suffering from an active case of the illness [32] [33]

1.2.6 Miliary TB

Miliary TB is a rare but severe form of TB. It occurs when the bacteria Mycobacterium tuberculosis spreads throughout the body via the bloodstream, resulting in the development of microscopic, seed-like nodules (known as milia) in various organs and tissues, including the lungs, liver, spleen, bone marrow, and lymph nodes. These nodules can cause inflammation and damage to the affected organs or tissues, and can interfere with the normal functioning of the immune system. Miliary TB symptoms may include fever, night sweats, weight loss, cough, breathing difficulties, weariness, stomach discomfort, and jaundice, depending on the organs affected. Miliary TB can cause organ failure, sepsis, and even death in severe cases. Miliary tuberculosis can be fatal if not treated immediately. According to a review of TB epidemiology, Miliary TB accounts for less than 1% of all TB cases [34]. Miliary TB can

occur in people who have just been infected with TB as well as those who have had latent TB for many years. Those with weakened immune systems, such as those with HIV/AIDS, cancer, or receiving immunosuppressive medication, are more likely to develop Miliary TB. Miliary TB can occasionally arise as a complication of untreated or ineffectively treated active TB disease. Medical history, physical examination, laboratory testing, and imaging techniques such as chest X-rays, CT scans, and ultrasounds are frequently used to diagnose Miliary TB. Blood, urine, or other bodily fluids are typically used to culture the TB bacteria to provide a conclusive diagnosis. Miliary TB is a dangerous condition that needs to be identified and treated very away. It is crucial to get tested for TB and get medical assistance if you have recently come into touch with someone who has active TB disease or if you are experiencing symptoms that could indicate TB [35] [36].

1.2.7 Skeletal TB

Skeletal tuberculosis is also known as bone and joint tuberculosis or osteoarticular tuberculosis. It primarily affects the joints and bones. It accounts for about 1-3% of all TB cases [37]. Skeletal TB symptoms depend upon the affected site and the stage of the disease. Some common symptoms are bone pain, swelling and deformity, pus formation, and constitutional symptoms. It is very challenging to diagnose skeletal TB because its symptoms can be similar to other bone and joint disease conditions. Therefore, a detailed medical evaluation such as medical imaging and microbiological tests of the affected site is very necessary [38].

1.2.8 Genitourinary TB

Genitourinary TB usually occurs due to the spread of Mycobacterium tuberculosis bacteria from a primary pulmonary infection. Through the bloodstream, the bacteria can reach the genitourinary system. It can also be spread through sexual contact with an infected person. Genitourinary TB symptoms depend upon the affected organ and the stage of the disease. In the case of urinary TB, symptoms may include pain and discomfort during urination, blood in the urine, and frequent urination. If bacteria infect the genital organ, in males, pain or swelling in the testicles or prostate gland may occur. In females, symptoms may include menstrual irregularities, pelvic pain, or vaginal discharge. Kidney TB can lead to symptoms such as fatigue, fever, weight loss, flank pain, and night sweats. While these types of TB are relatively

rare, they can still occur, particularly in people with weakened immune systems or those who have not received appropriate treatment for TB. Treatment for these types of TB is often more complex and may require a combination of different antibiotics over a longer period than standard TB treatment. It's important to note that TB is a highly treatable and curable disease, but early detection and treatment are essential to prevent the spread of the disease and prevent more severe forms of TB from developing [39] [40].

1.3 Diagnosis of Tuberculosis

Diagnosis of TB is very important for timely treatment, prevention of transmission, and reduction of TB-related morbidity and mortality. Improving the efficiency and early and accurate diagnosis of tuberculosis aids in the effectiveness of treatment [41]. Some TB diagnosis tests take a long time to get a result, while others are inaccurate. The most accurate tests based on culture tests take a long time to complete. Some new highly accurate TB diagnosis methods based on molecular analysis such as the GeneXpert test and the TrueNat test are very expensive and require complex laboratory facilities and these tests are rarely available in developing countries. There are several tests available for diagnosing tuberculosis (TB). The most commonly used tests include the TB skin test, TB blood test, GeneXpert MTB/RIF, sputum test, and medical imaging [42] [43].

1.3.1 TB Skin Test

The TB skin test, commonly known as the Mantoux tuberculin skin test, is a diagnostic process used to identify whether a person has mycobacterium tuberculosis. In a Tuberculosis skin test, a little amount of pure protein derivative (PPD) is injected into the skin, usually on the forearm, as part of the test, and after 48–72 hours, the area of injection is checked to see if a raised, red bump has appeared [44]. While the TST can be a useful tool for detecting TB infection, there are several drawbacks to the test that should be considered:

False positive: A person may test positive for TB infection even if they do not have active TB disease since the TST has the potential to give false positive results. Those who have received the BCG vaccine or who have been exposed to other mycobacteria that are related to the TB bacterium may develop this condition.

False negative**:** The TST has the potential to yield false negative results, which means that someone could test negative for TB infection even while they have active TB disease. Those with weakened immune systems, such as those who have HIV or certain autoimmune illnesses, may experience this.

Limited specificity: The TST is not TB-specific, thus it can produce a positive result in people who have been exposed to other mycobacteria that are not TB or who have previously had TB infections that have been successfully treated.

Interpretation challenges**:** A trained healthcare professional is required to correctly interpret the TST results. To determine whether the test is positive or negative, the size of the raised, red bump at the injection site must be measured and compared to established standards.

Delayed results: The TST has a 48–72 hour waiting time before results are available as the patients have to check the doctor after 2 or 3 days to see whether they reacted injecting TB protein, which can be inconvenient for some people and delay the treatment for those who test positive.

Thus, the TB skin test is not very accurate as it has several limitations. Healthcare providers may use alternative tests, such as interferon-gamma release assays (IGRAs) and medical imaging (chest x-rays, CT Scans, etc.) to overcome some of these limitations.

1.3.2 TB Blood Test

Blood tests for TB are also referred to as IGRAs (interferon-gamma release assays. TB blood tests or IGRAs measure a person's immune system response to the TB bacteria by observing the release of interferon-gamma from T-cells in response to particular TB antigens. Compared to the conventional tuberculin skin test, the Tb blood test has several benefits (TST). The Tb blood test, in contrast to the TST, requires only a single visit, provides results in a day or two, and is unaffected by prior Bacilli Calmette-Guérin (BCG) vaccination. The Tb blood test is also more accurate than the TST because it is less likely to yield false-positive findings in people who have received the BCG vaccine or who have been exposed to mycobacteria that are not associated with TB. However, there are several limitations to the Tb blood test that should be considered when interpreting the results. The test cannot distinguish between latent tuberculosis infection (LTBI) and active tuberculosis sickness. To identify the

presence of active TB illness, additional clinical and radiological assessment is required. Secondly, people with weakened immune systems, such as those with HIV or those using immunosuppressive drugs, may receive false-negative test results. Moreover, this test might not be accessible in all healthcare settings, especially in low-resource countries and it is more expensive than the TST [45] [46].

1.3.3 Sputum Test

A sputum culture test is a laboratory procedure that is used to determine whether Mycobacterium tuberculosis (MTB) is present in a patient's sputum sample. A sample of sputum or mucus spat up from the lungs, is taken for the test and placed in a culture medium that supports the growth of MTB bacteria. If MTB bacteria are present in the sample, they will grow in the culture media and can be found and subjected to additional examination. Due to its ability to identify even minute quantities of MTB bacteria, the sputum culture test is regarded as the gold standard for TB diagnosis [47]. Also, it is more trustworthy than other diagnostic procedures like the sputum smear test, which could produce negative results. The sputum culture test, however, has several drawbacks, including:

Delayed results: The sputum culture test can take several weeks to generate results, delaying the start of treatment and increasing the risk of spreading the infection to others.

Limited sensitivity: If the sample is too small, the bacteria are dormant, or the patient has an infection with a strain of MTB that is resistant to the antibiotics used in the culture medium, the sputum culture test might not be able to detect MTB bacteria.

False-negative results: If the sample is contaminated or the bacteria do not grow in the culture media, the sputum culture test may occasionally produce a false negative result.

Invasive sample collection: Some patients may find it challenging to collect a sputum sample, especially those who are unable to cough up enough sputum or who have a weak cough.

High cost: The cost of the sputum culture test can be high; approximately 6000 Pakistani rupees, especially in low-resource countries where laboratory equipment and supplies may be limited.

Lack of specificity: Even though the sputum culture test is quite specific for MTB bacteria, it can also pick up non-pathogenic mycobacterial species, giving false positive results.

1.3.4 GeneXpert MTB/RIF test

A molecular diagnostic test called the GeneXpert MTB/RIF test is used for the diagnosis of tuberculosis (TB) and resistance to the antibiotic rifampicin, a crucial first-line treatment for TB. A small amount of sputum (phlegm coughed up from the lungs) or other respiratory specimens are used in the test, and they are processed using a unique cartridge that contains reagents and probes for the detection of TB DNA. In comparison to traditional TB diagnostic techniques, the GeneXpert MTB/RIF test provides several benefits, including quick results (within 2 hours), excellent sensitivity and specificity, and the capacity to concurrently detect rifampicin resistance. These characteristics make the test especially helpful in situations when timely diagnosis and treatment of TB are essential, such as in places with limited resources and a high TB prevalence or in people who are co-infected with HIV. However, The GeneXpert MTB/RIF test has significant limitations. One major limitation is that this test is very expensive and due to the expensive nature of the test, it can be prohibitive in low-income countries. Furthermore, the test may produce false-negative results in individuals with low bacterial burdens or extra-pulmonary TB, which can result in missed diagnosis and delayed treatment. False-positive outcomes can also happen, especially in patients who have already received TB treatment or who have non-tuberculous mycobacterial infections. The GeneXpert MTB/RIF test's failure to identify resistance to antibiotics other than rifampicin is another drawback. Further testing may be necessary when resistance to other antibiotics is known or suspected [48] [49]. Furthermore, the test requires sophisticated laboratory equipment and qualified employees, which may not be available in all settings, especially in low-income countries.

1.3.5 Medical imaging

The importance of medical imaging in TB has increased exponentially. Imaging plays an essential role in the prediction and management of TB disease. Several imaging techniques are used to predict TB, such as X-rays, Positron emission tomography scans, Magnetic resonance imaging (MRI), Computed Tomography (CT) scans, and ultrasound. Chest X-rays are the most widely used and basic imaging modality for pulmonary TB. Computed

Tomography (CT) scans, Magnetic resonance imaging (MRI), Positron emission tomography scans, and ultrasound are helpful in the diagnosis of extra pulmonary as well as pulmonary TB, but these techniques are not widely used due to their higher cost as compared to chest X-rays, especially in low-income countries**.** Chest X-rays are most commonly used in the diagnosis of tuberculosis (TB) as they can show distinctive changes in the lungs caused by the disease. World health organization also recommends chest X-rays as a screening tool for TB [50]. Mycobacterium tuberculosis, the bacterium that causes TB, mainly affects the lungs but can also affect other regions of the body. The chest X-ray is a non-invasive imaging procedure that produces images of the chest region, including the lungs, heart, and other structures in the chest, using low levels of radiation. Chest X-rays are easily accessible and quick to perform. This is particularly crucial in regions where TB is widespread since timely identification and treatment can stop the disease's spread. Chest X-rays are particularly useful for detecting pulmonary TB, the most common type of tuberculosis and it accounts for about 85% of all TB cases worldwide. The images can reveal recognizable lung alterations such as nodules, cavities, and infiltrates. Chest X-rays can also be used to track how TB develops over time. This can be useful for determining any problems and the success of the treatment. Some patients may be concerned about the minimal levels of radiation exposure involved with chest X-rays. However, the amount of radiation exposure is generally considered safe and the benefits of early diagnosis and treatment of TB usually outweigh the risks [51]. However, diagnosis by chest X-rays has some limitations. One major limitation is that TB chest X-rays are often misclassified to some other diseases of similar radiological patterns such as covid-19 [52], which may lead to the wrong medication for the patients. Moreover, diagnosis by chest X-ray images is limited by the need for expert radiologists to accurately identify tuberculosis disease [53].

1.4 Deep Learning in tuberculosis diagnosis

Deep learning approaches have shown promising results and success in various aspects of disease prediction and medical imaging. When it comes to tuberculosis prediction, the employment of deep learning techniques is becoming more frequent, contributing to improved efficiency and accuracy in the prediction and classification of TB disease. Deep learning can be used as an auxiliary tool to help medical professionals in the prediction of TB disease. By using deep learning algorithms, a medical expert may attain help in the diagnosis of TB

disease. Figure 1.1 illustrate a potential framework for getting a deep-learning solution for the prediction of tuberculosis disease.

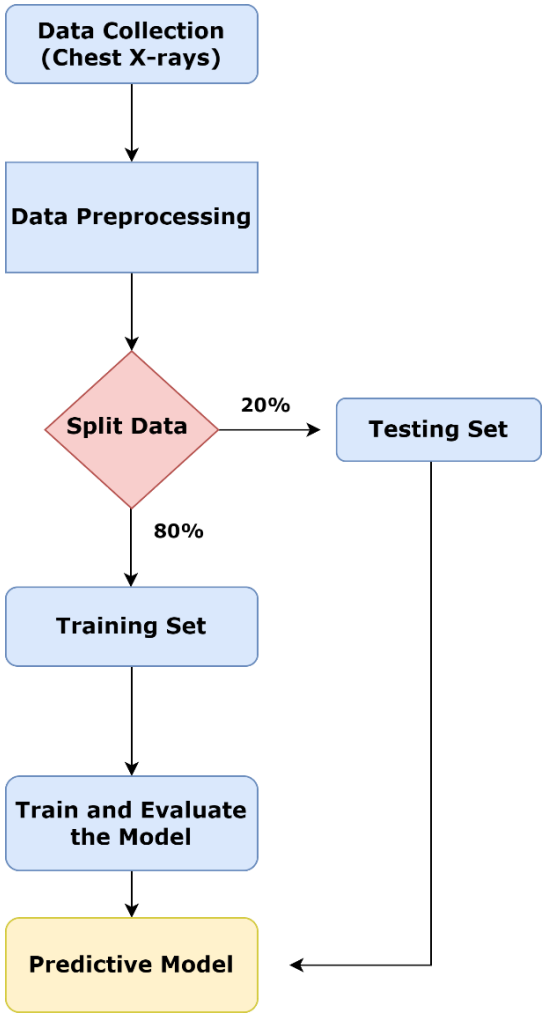

Figure 1.1: A potential framework for getting a deep-learning solution for the prediction of tuberculosis disease

1.5 TB Diagnosis in low-resource countries

In low-resource countries, TB diagnosis is very important where the disease is most prevalent and resources for diagnosis and treatment are often limited. In 2020, 87% of new TB cases occurred in the 30 high TB burden countries [54]. Eight countries; India, Pakistan, Indonesia, the Philippines, Bangladesh, China, Nigeria, and the Democratic Republic of the Congo accounted for more than two-thirds of the global total. In these circumstances, chest X-rays are an important prediction tool for the diagnosis of TB, as they are widely accessible,

relatively inexpensive, and capable of revealing valuable information about the extent and severity of the disease. One of the major advantages of using chest X-rays for the diagnosis of TB in low-resource countries is that they can be performed quickly and easily, even in remote areas with limited resources. This is particularly important in regions where access to more advanced diagnostic techniques, such as computed tomography (CT) scans, may be limited or unavailable. Furthermore, chest X-rays can aid in the detection of TB cases that could otherwise go undetected, particularly in settings where other diagnostic techniques, such as sputum microscopy or culture, may be less accurate or specific. Chest X-rays in particular can aid in the detection of extra-pulmonary TB, which affects organs other than the lungs and can be more challenging to diagnose. Last but not least, chest X-rays can provide important information regarding the severity of TB and the extent of lung damage, which can assist determine treatment decisions and track the development of the illness over time. This information can be very helpful in low-resource settings, where resources for follow-up and monitoring may be limited.

1.6 Economic burden on Pakistan due to tuberculosis (TB) disease

The Eastern Mediterranean Region (EMR) accounted for 8.3% of the total number of TB cases reported by the World Health Organization (WHO), Pakistan ranked fifth among the 30 nations with the highest burden of TB and contributed 5.8%, carrying almost 69% of the TB burden in the Eastern Mediterranean Region (EMR) [55]. In well-known hospitals in Pakistan, the cost of tuberculosis (TB) tests for individuals aged 11 years and above ranges between 10,000 and 11,000 Pakistani Rupees. For individuals below 11 years of age, the cost typically falls between 8,000 and 9,000 Pakistani Rupees. These prices may vary depending on the specific hospital and location within Pakistan [56]. In government hospitals, the cost of TB tests is very low but the healthcare system is ineffective. Numerous flaws exist, including a lack of management, a lack of expert and trained radiologists and doctors especially in remote areas, a lack of resources, poor quality laboratories, and a lack of leadership.

1.7 Problem Statement

CXR images are most commonly used in the diagnosis of tuberculosis. However, the use of CXR images for the prediction of tuberculosis (TB) is limited by the need for trained and expert radiologists or pulmonologists and there is also a lack of trained medical

professionals and high-quality labs, especially in remote areas of Pakistan. Moreover, CXR images are often, misclassified to some other pulmonary diseases of similar radiological patterns, such as COVID-19, and pneumonia which may lead to wrong medication and delayed treatment of the disease.

1.8 Objectives

The following are the research objectives of this study:

- Collect a diverse dataset of CXR images focusing on TB cases from a local hospital.
- Develop a deep learning model capable of accurately predicting tuberculosis disease based on CXR images, in a time-efficient and cost-effective way.
- Develop an *in-house* deep-learning based user friendly web application for the prediction of TB disease in the Pakistani population.

CHAPTER 2
LITERATURE REVIEW

2. Literature Review

2.1 Misdiagnosed cases

Tuberculosis (TB) is a bacterial infection that affects the lungs and can cause symptoms including fever, cough, and weight loss. However, the symptoms of TB can be similar to those of other pulmonary diseases, such as covid-19 or pneumonia. Due to similar symptoms and radiological patterns, Tuberculosis can be misdiagnosed as covid-19 or pneumonia, etc. Misdiagnosis of TB as covid-19 or vice versa can have serious effects on patient management and public health. Many studies have reported Tuberculosis cases being misdiagnosed to other pulmonary conditions because of similar symptoms and radiological findings. Based on symptoms and radiological presentations, about 34% of the patients with microbiologically proven TB were initially classified as covid-19 during the covid-19 pandemic [57]. Similarly, in a research study, TB cases were found to have been misdiagnosed as covid-19 and pneumonia because of similar chest X-ray results [58]. Another research study was conducted to determine how tuberculosis misdiagnoses occurred in India during the covid-19 pandemic. To prevent misdiagnosis, the scientists discovered that patients who were initially diagnosed with COVID later had tuberculosis. This finding emphasizes the need to carefully evaluate respiratory symptoms and use the right diagnostics tools [59]. Additionally, there have also been cases where covid-19 was incorrectly identified as TB. According to a study conducted, a significant proportion of covid cases were initially diagnosed with tuberculosis (TB) due to their clinical symptoms and chest X-ray results [60]. In another study, a patient is described who was initially thought to have covid-19 based on clinical signs and evidence on a chest X-ray, but who was later shown to have pulmonary tuberculosis. In this study, the authors emphasize the significance of including tuberculosis in the differential diagnosis for patients exhibiting respiratory symptoms, especially in regions where tuberculosis is common [61]. The researchers determined the clinical traits of patients with pulmonary tuberculosis who had initially received the incorrect diagnosis of pneumonia at the emergency room. The researchers discovered that patients with tuberculosis were more likely than those with pneumonia to experience longer-lasting coughs, weight loss, and night sweats. The study emphasizes the necessity of cautious symptom evaluation and appropriate diagnostic tests to prevent misdiagnosis [62]. These misdiagnosis cases highlight the importance of accurate and timely diagnosis of TB.

2.2 Need of an early and accurate diagnosis

There is a need for accurate and early diagnosis of tuberculosis (TB) because tuberculosis (TB) is a highly contagious disease that can spread via the air when an infected person coughs or sneezes. TB must be diagnosed accurately and quickly for several reasons. First, TB can be stopped from spreading to other people with early diagnosis and treatment. Second, early treatment can increase the likelihood of a full recovery and lower the danger of major health issues. Moreover, it will reduce the tuberculosis misclassification rate to other pulmonary diseases. Finally, a correct diagnosis can guarantee that patients receive the right treatment and avoid treatments that are not necessary and can lead to drug resistance.

2.3 Role of Chest X-Rays in the Diagnosis of Tuberculosis

Chest X-rays are very important for the diagnosis and treatment of tuberculosis (TB) disease. They are used to recognize distinctive abnormalities in the lungs such as cavities, nodules, and infiltrates that point to the presence of tuberculosis (TB). Chest X-rays can also be used to assess a patient's response to treatment and track the progression of the disease. Generally, in low-resource countries, Chest X-rays are most commonly used for the diagnosis of tuberculosis [63], especially in remote areas where resources are limited and tests like culture and GeneXpert cannot be performed as they are expensive and require high-resource laboratory conditions. Several studies in recent years have emphasized the importance of chest X-rays in the diagnosis of TB disease. For example, a study published in 2023 found that, for the y detection and treatment, it is important for doctors or radiologists to recognize and identify the visual signals of active tuberculosis from CXR [64]. Similarly, according to a study published in the journal PLOS ONE [65], chest X-rays were found to be a useful tool for predicting the risk of progression from latent TB infection to active TB disease in a population of healthcare workers in South Africa. According to the study, people with abnormal chest X-rays had a much higher chance than people with normal chest X-rays of developing active tuberculosis over the course of two years. Another study published in the journal Clinical Infectious Diseases examined the diagnostic efficacy of chest X-rays for the diagnosis of TB disease in a population of Nairobi, Kenya [66]. The study demonstrated that chest X-rays showed a high sensitivity for TB disease diagnosis, especially when combined with other diagnostic tests like sputum smear microscopy and culture. Moreover, the World Health Organization (WHO) also suggests using chest X-rays as part of the diagnostic

process for TB disease [67]. In situations where other diagnostic methods, such as sputum smear microscopy and culture, may not be available or may be less sensitive, chest X-rays are very helpful.

The use of chest X-rays should be taken into consideration in all patients with a suspected or confirmed TB infection since they play a very important role in the diagnosis and management of TB disease. However, it is important to note that chest X-rays should always be performed in conjunction with other diagnostic tests such as sputum smear microscopy as chest X-rays alone are insufficient to diagnose TB disease.

2.4 Existing deep learning models for tuberculosis diagnosis:

Ahmed et al. developed a unique TB-UNet for reliable segmentation of lung regions that are based on dilated fusion block (DF) and Attention block (AB) blocks. They achieved the top results in terms of Precision (0.9574), Recall (0.9512), F1 score (0.8988), IOU (0.8168), and accuracy (0.9770). For the accurate classification of chest x-rays images of tuberculosis, they presented TB-DenseNet, which is based on five dual convolution blocks, a DenseNet-169 layer, and a feature fusion block. They used three chest X-ray datasets to perform the experiment and original images were fed to TB-DenseNet for improved classification. Also, the proposed technique is tested simultaneously against three different diseases, including COVID-19, tuberculosis, and pneumonia. The best outcomes are obtained for Precision (0.9567), Recall (0.9510), F1 score (0.9538), and Accuracy (0.9510) [68]. Goram et al. proposed a deep learning (DL) architecture for multi-class classification of COVID-19, lung opacity, lung cancer, tuberculosis (TB), and pneumonia. To meet the DL requirements, they resized, normalized, and randomly split the CXR images of 10,192 normal, 20,000 lung cancer images, 20,000 lung opacity images, 5870 pneumonia images, 3615 COVID-19 images, and 6012 lung opacity images. To classify data, they used a pre-trained model called VGG19, followed by three blocks of a convolutional neural network (CNN) for feature extraction and a fully connected network for classification. With 96.48% accuracy, 93.75% recall, 97.56% precision, 95.62% F1 score, and 99.82% area under the curve, their experimental results demonstrated that suggested VGG19 + CNN surpassed other work (AUC) [69]. Abdullahi et al. described automated tuberculosis and non-tuberculosis case differentiation utilizing pre-trained Alex Net Models on X-ray and microscope slide pictures. The study used microscopic slide photos from both the Kaggle repository and the Near East University

Hospital, as well as a chest X-ray dataset that was publicly available on Kaggle. The model produced results for 70:30 splits with 90.56% accuracy, 97.78% sensitivity, and 83.33% specificity for the classification of tuberculosis using microscopic slide pictures. The model scored 93.89% accuracy, 96.67% sensitivity, and 91.11% specificity for 70:30 splits when classifying tuberculosis using X-ray images [70]. In a study [71], researchers proposed a CNN-based transfer learning-based method for automatically interpreting pulmonary diseases from chest X-rays, such as Covid-19, tuberculosis, nodules, and pneumonia. The explanation job includes radiographs of COVID-19 because pneumonia, one of the lung disorders that it produces, is fatal. With the help of the COVID-CT dataset and the COVIDNet dataset, they extensively trained the ResNet50 neural network. The interpretation of the classification results was done using the interpretable model LIME. Marios et al. [72], analyzed five deep-learning models to classify COVID-19 from chest X-ray images. Their study's objective is to demonstrate the value and potential of specific deep-learning models in COVID-19 CXR images. They used 11,956 images of coronavirus-positive patients, non-COVID-19 contains 11,263 images of viral or bacterial pneumonia patients and normal contains 10,701 healthy images. More specifically, they used Transfer Learning and ResNet50, ResNet101, DenseNet121, DenseNet169, and InceptionV3. On the largest publicly accessible resource for COVID-19 CXR images, all models were tested and trained. Additionally, they were assessed using unidentified data that was not utilized for training or validation, validating their performance and defining how they should be used in a medical setting. All models performed satisfactorily, with ResNet101 outperforming the others by scoring 96% in Precision, Recall, and Accuracy. Mohan et al. [73], proposed a model for the classification of CXR Images into COVID-19, Pneumonia, and Tuberculosis. 7132 chest x-ray (CXR) images from publically accessible datasets were used to validate the proposed model. Gradient-weighted Class Activation Mapping (Grad-CAM), Local Interpretable Model agnostic Explanation (LIME), and Shapley Additive Explanation (SHAP) are also used to interpret and explain the results to make them more understandable. Convolution features were initially extracted to gather detailed object-based data. The black-box method of the DL model was then explored using shapely values from SHAP, predictability findings from LIME, and heatmap from Grad-CAM, yielding average test accuracy of 94.31 1.01% and validation accuracy of 94.54 1.33 for 10-fold cross-validation. Vinaya kumar et al. [74], suggested a multichannel deep-learning method for chest X-ray-based lung disease identification. EfficientNetB0, EfficientNetB1, and EfficientNetB2 pre-trained models are the

multichannel models employed in this study. The characteristics of EfficientNet models were combined. The fused characteristics were then sent via many completely connected non-linear layers. The features were then fed into a classifier for lung disease diagnosis using stacked ensemble learning. Random forest and SVM were used in the first stage of the stacked ensemble learning classifier for lung disease detection, while logistic regression was used in the second stage. The effectiveness of the suggested technique was examined in depth for several severe lung diseases, including pneumonia, TB, and COVID-19. The results of the proposed approach for using chest X-rays to detect lung diseases including pneumonia, TB, and COVID-19 were compared with those of similar methods to demonstrate that the proposed method is reliable and capable of producing improved results. The overall detection accuracy of the suggested approach was 98% for pediatric pneumonia lung disease, 99% for TB lung disease, and 98% for COVID-19 lung illness. In a study [75], researchers proposed two methods for classifying TB disease using data from X-rays. To classify the disease as TB images and normal images, they first used handmade features in a basic neural network with Support Vector Machine (SVM). They designed an ANN system for 13 input neurons, 10 hidden neurons, and 2 output neurons to train features, which were fed as input to SVM for classification. The experimentation was done on MATLAB 2014b. When all features were fed into an ANN-SVM-based classification algorithm, accuracy was 94.6%. The second methodology we used to classify the TB disease was deep learning, which can train high-level features from datasets as opposed to handmade feature methods. In which they created a deep convolutional neural network for binary classification (DCNN). Google Collab notebooks were used to model DCNN with GPU-based Keras library and Tensor flow as the back end. The TB Chest X-ray dataset used in the experiments was collected from the Kaggle community, and the results indicated a classification accuracy of 99.24%. **Table 2.1** presents a brief summary of different research studies proposed for the classification of tuberculosis. The table includes the publication year, models used for the classification of tuberculosis, accuracy achieved, size of the dataset employed and limitations encountered.

Table 2.1: Literature Review of Tuberculosis Classification Studies using CXR images: Method, Accuracy, Datasets and Limitations Examined

Sr.	Authors (Year)	Method	Accuracy	Dataset Size	Limitations
1	Jung Liu et al. (2023) [76]	CNN	90%	TB: 500 Normal: 1000	Class Imbalanced
2	Huy et al. (2023) [77]	Customized CNN	98%	TB: 1094 Normal: 3906	Class Imbalanced
3	Margarat et al. (2022) [78]	Deep Belief Network (DBN)	99%	TB: 416 Normal: 384	Limited data
4	Fati, S.M et al. (2022) [79]	Res-Net-50, GoogLeNet, SVM	99%	TB: 1036 Normal: 3826	Class Imbalanced
5	Antony et al. (2022) [80]	Bayesian CNN	90%	TB: 416 Normal: 384	Limited Data
6	Ibrahim et al. (2022) [81]	AlexNet+SVM	98%	TB: 416 Normal: 384	Limited Data
7	Pavani et al. (2021) [82]	Naïve Bayes classifier (NBC)	95%,	TB: 416 Normal: 384	Limited data
8	Ayaz et al. (2021) [83]	CNN	97%	TB: 416 Normal: 384	Limited data
9	Vajda et al. (2018) [84]	DNN	97%	TB: 416 Normal: 384	Limited data

CHAPTER 3
METHODOLOGY

3. Methodology

Deep learning approaches are used to predict tuberculosis disease from chest X-rays. This section provides a comprehensive description of the employed dataset, pre-processing of the dataset, applied classifier, and evaluation of the classifier. Figure 3.1 illustrates the methodology used in the proposed study.

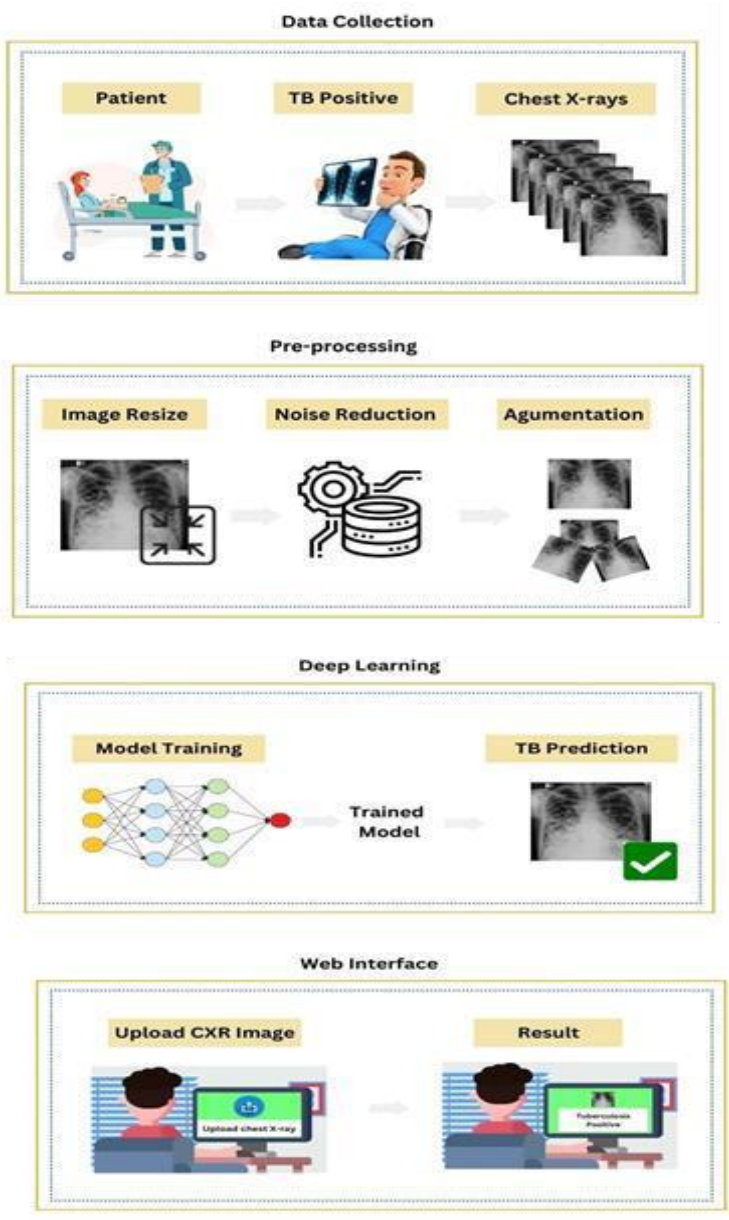

3.1 Methodology workflow used in this study

3.1 Dataset Description and Pre-processing

Deep learning requires a large and diverse dataset to train the model. The quality and quantity of the data are essential factors and play an important role in the performance and accuracy of the learning model. A large dataset helps the model learn more diverse features and patterns and performs well on unseen data. Moreover, a diverse dataset that includes different variations of the target output, such as different angles, colors, and backgrounds of images, helps the model to classify images in real-world problems accurately. In this study, 7539 CXR images were used to experiment. Table 3.1 summarizes the number of data used in this study. A total of 2500 TB CXR, 22 COVID-19 CXR images and 517 normal CXR images were collected from a well-known hospital in Pakistan, Syed Muhammad Hussain TB Sanatorium, located in Samli. The TB CXR images are collected from a diverse range of tuberculosis patients to ensure the representation of different disease patterns and imaging conditions. To address the class imbalance issue, 2000 normal chest X-rays were also collected from Kaggle[85]. The sample images of tuberculosis and normal are shown in Figure 3.2 and Figure 3.3. For COVID-19, 2500 CXR images were also collected from Kaggle[86], a popular open-source platform for sharing datasets. The sample images of COVID-19 and normal are shown in Figure 3.4.

Table 3.1: Summary of numbers of data that are applied in this study

Data	Number of CXR images
Tuberculosis	2500
COVID-19	2522
Normal	2517

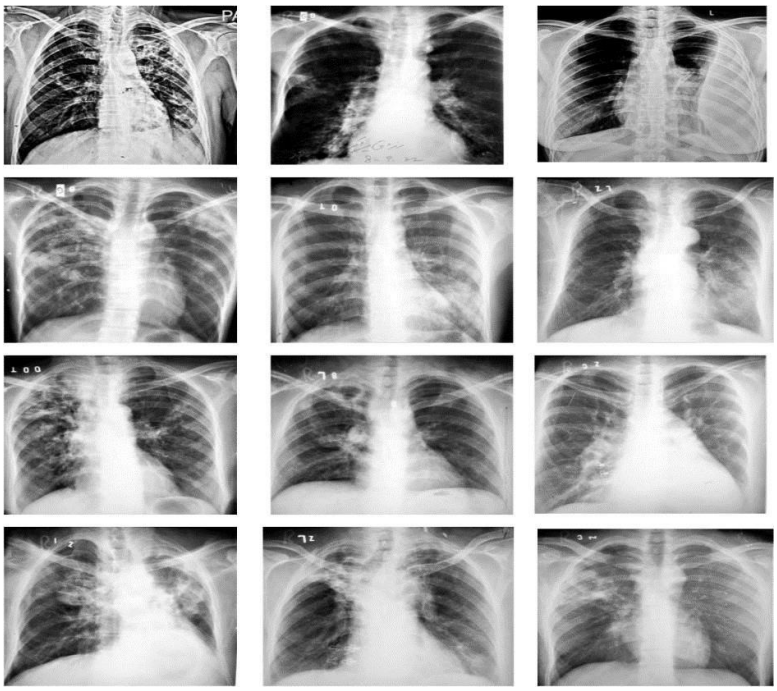

Figure 3.2: Sample images of Tuberculosis

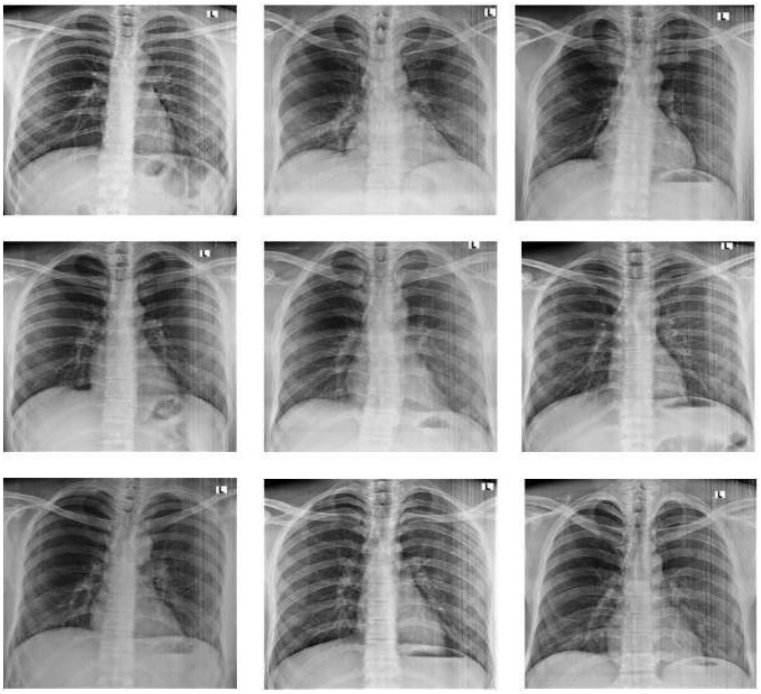

Figure 3.3: Sample images of Normal

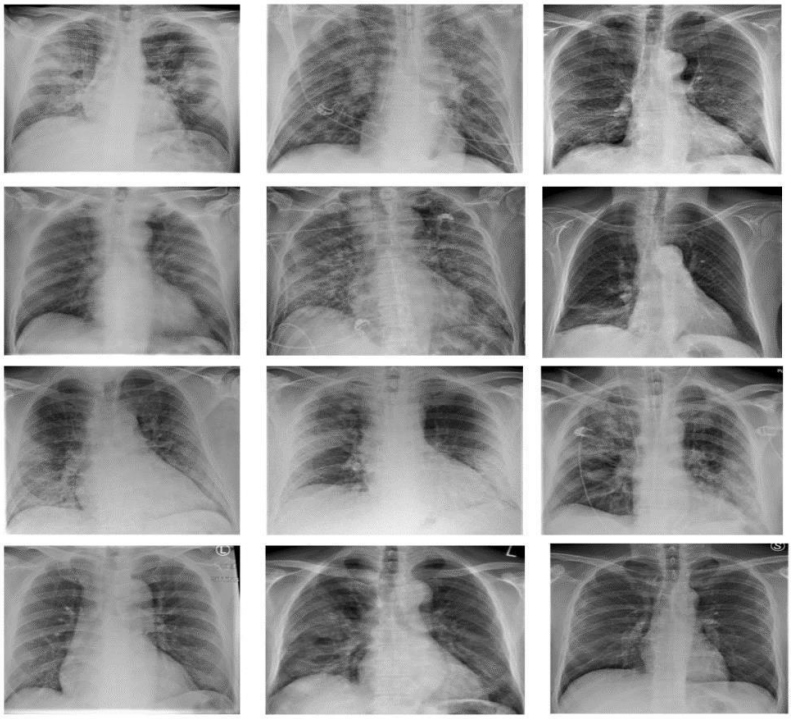

Figure 3.4: Sample images of COVID-19

After the data collection, several pre-processing techniques are carried out on the images to enhance the quality and suitability of the data for the proposed deep learning model. Resizing the images to a consistent size is an essential step in deep learning models. Image resizing ensures that all the images have the same dimensions. In this study, to prepare the dataset for the model, all the CXR images are resized to 256×256 to meet the input dimension of the proposed model. After resizing the images to a fixed size of 256×256, the Contrast Limited Adaptive Histogram Equalization (CLAHE) technique was implemented to enhance the contrast of the images and enhance the visibility of important features and details in chest x-rays. Figure 3.5 shows CXR images before and after applying the CLAHE. Data augmentation was also applied to CXR images to artificially increase the dataset size and diversity of the dataset by applying various transformation and modification techniques to existing tuberculosis, normal, and COVID-19 CXR images and to enhance the ability of the model to deal with different pattern variations in the chest X-ray images in real-world scenarios. We used a rotation range of 10, a width shift range of 0.1, a height shift range of 0.1, a zoom range of 0.1, and horizontal/vertical filliping to perform image augmentation. This approach resulted in a more robust and accurate model, providing an improved multi-classification of CXR images. As the deep learning model deals with numerical data, all the

images of the dataset were converted into arrays before using them as input for the model. Three class labels used in the study are TB, normal, and COVID-19. To use these labels as input for the model, we assigned numerical values to these class labels and assign the value 1 to the TB label, the value 2 to the COVID-19 label, and the 0 value to the normal label. These labels were used as output targets during the model training process. To experiment, the dataset was divided into two subsets, a training subset that contained 80% of the total images and a testing subset that contained 20% of the total images.

3.2 Model Architecture

Python 3.8 and Google collab notebook were used for the development of the deep learning model. The architecture of the CNN model is shown in Figure 1. The first layer is the input layer which takes the CXR image of size 256 * 256 * 3 as an input. The second layer is the convolutional 2D layer with 32 filters. The filter size of this layer is 3×3 followed by activation function ReLU and 2×2 max pooling layer. This third layer is a convolutional layer with 64 filters. The filter size of this layer is 3×3 followed by activation function ReLU and 2×2 max pooling layer. The fourth layer of the model architecture is a convolutional layer with 128 filters. The size of the filter of this layer is 3×3 followed by activation function ReLU and 2×2 max pooling layer. The fifth layer is a convolutional layer with 128 filters. The size of the filter is 3×3 followed by activation function ReLU and 2×2 max pooling layer. The sixth layer is a flatten layer. Next two dense layers are used. A dropout layer with a rate of 20% is also applied after first dense layers to avoid overfitting. The last layer or the second dense layer of the architecture followed by a softmax function classify the image into three categories. The output shape and the learning parameters of the CNN are shown in Table 3.2.

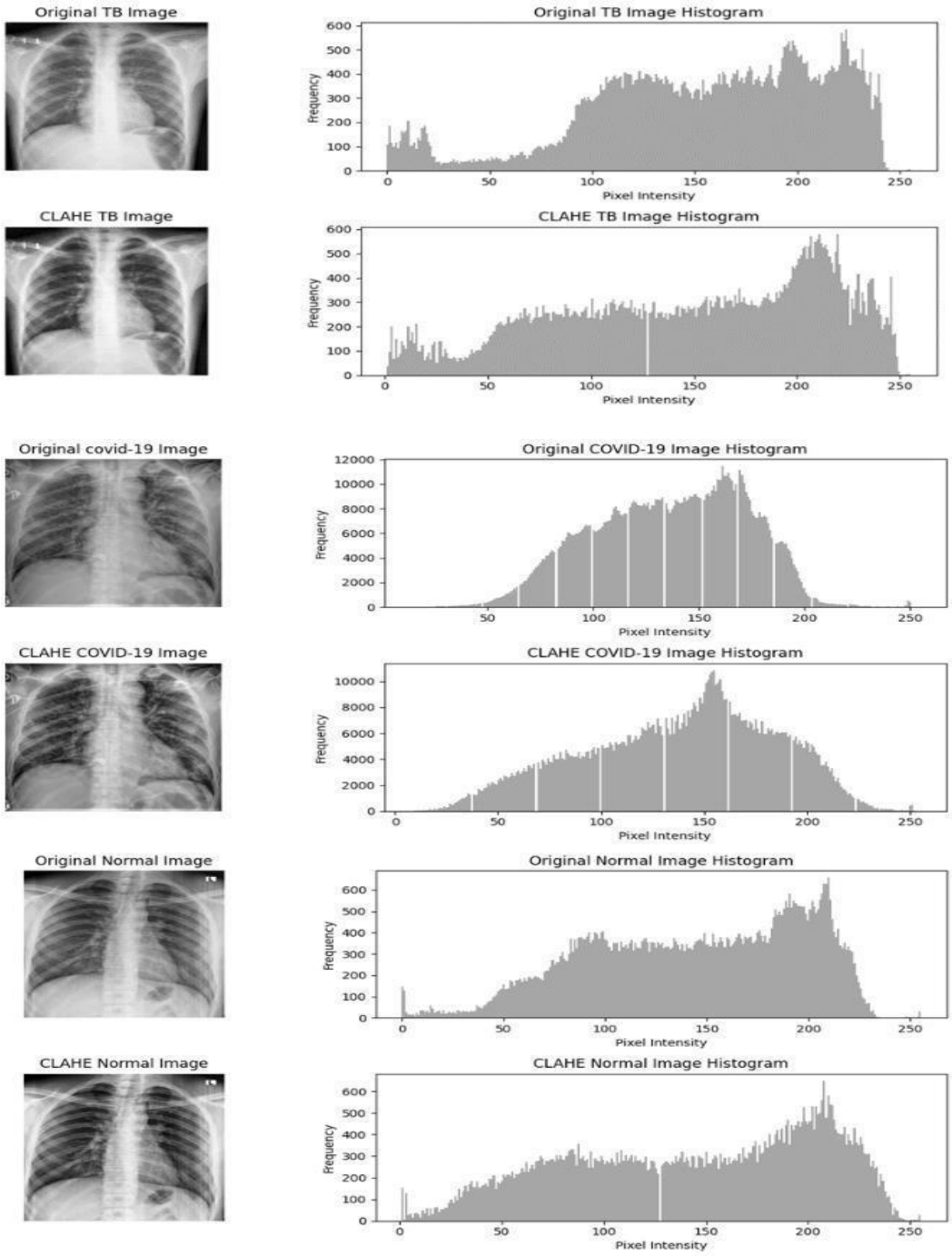

Figure 3.5: CXR image before and after applying CLAHE

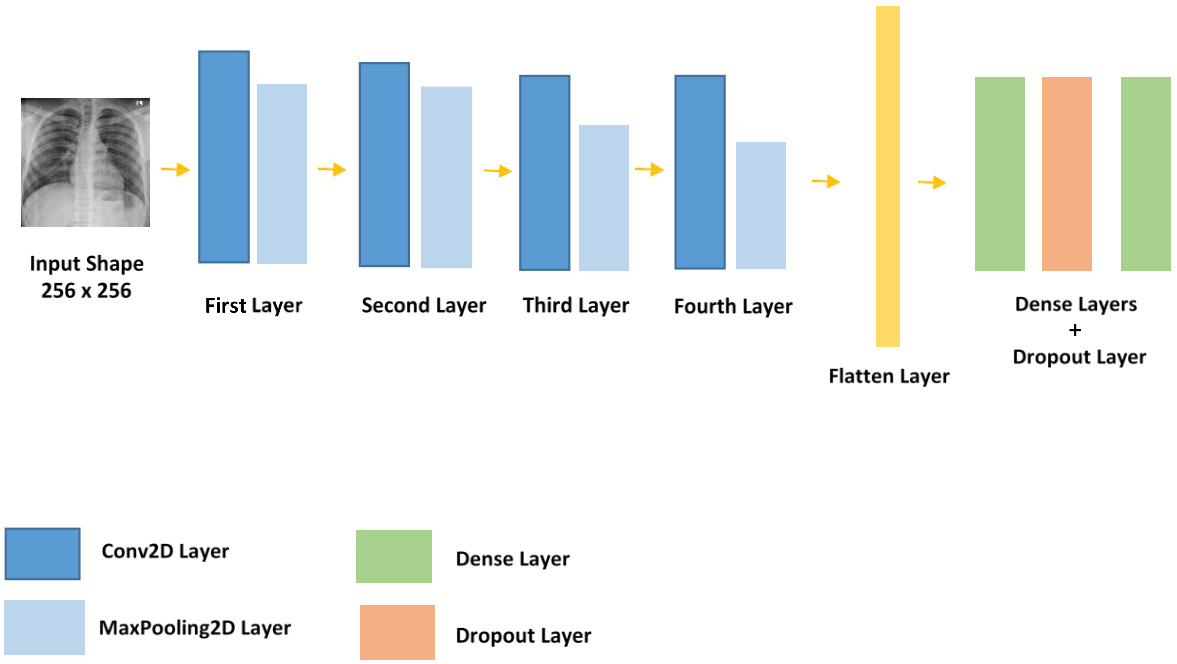

3.6: Architecture of the Model

Table 3.2: Learning Parameters of the Model

No	Layer (type)	Output Shape	Parameters
1	conv2d (Conv2D)	(None, 254, 254, 32)	896
2	max_pooling2d(MaxPooling2D)	(None, 127, 127, 32)	0
3	conv2d_1 (Conv2D)	(None, 125, 125, 64)	18496
4	max_pooling2d_1(MaxPooling2D)	(None, 62, 62, 64)	0
5	conv2d_2 (Conv2D)	(None, 60, 60, 128)	73856

6	max_pooling2d_2(MaxPooling2D)	(None, 30, 30, 128)	0
7	conv2d_3 (Conv2D)	(None, 28, 28, 128)	147584
8	max_pooling2d_3(MaxPooling2D)	(None, 14, 14, 128)	0
9	flatten (Flatten)	(None, 25088)	0
10	dense (Dense)	(None, 512)	12845568
11	dropout_2 (Dropout)	(None, 512)	0
12	dense_1 (Dense)	(None, 3)	1539
Total Parameters		13,087,939	

3.3 Evaluation Methods

3.3.1 Confusion Matrices

A confusion matrix is commonly used to assess the performance of deep learning or any classification model. With the use of the confusion matrix, results may get a geed sense of whether or not findings are high performing as it provides a tabular representation of the predicted and actual class labels. Typically, a confusion matrix consists of four cells true positives, true negatives, false positives, and false negatives. In this proposed study, patients who are correctly classified as positive for either TB, normal or Covid-19 (true positives; TP), patients who were correctly classified as negative for TB, normal and COVID-19 (true negatives; TN), patients who were incorrectly classified as positive for three classes, when the actual class label was negative (false positives; FP), and patients who were incorrectly classified as negative while the actual class label was positive (false negatives; FN), were the elements of the confusion matrix. Predictions that turn out to be false negatives pose the greatest risk in the medical industry. Because the proposed study presented the classification of TB, normal, and COVID-19 which is a multi-

classification with three outcomes, we obtained a 3 X 3 matrix. By analysing the values of the confusion matrix, various performance parameters such as precision and recall etc. were calculated to determine the effectiveness of the model in classifying TB, normal and COVID-19.

Accuracy:

One indicator for assessing model performance is accuracy. Accuracy assesses the overall accuracy of the model's predictions. It is measured as the proportion of correct projections to total predictions.

$$\text{Accuracy} = \frac{\text{True Positives} + \text{True Negatives}}{\text{True Positives} + \text{True Negatives} + \text{False Positives} + \text{False Negatives}}$$

Precision:

Precision is determined as the ratio of the total number of true positives to the total number of instances predicted as positive.

$$\text{Precision} = \frac{\text{True Positives}}{\text{True Positives} + \text{False Positives}}$$

Recall

It is also known as sensitivity. The fraction of accurately predicted positive instances out of all actual positive instances is determined by recall. It is computed by dividing the total number of true positives by the total number of true positives and false negatives.

$$\text{Recall} = \frac{\text{True Positives}}{\text{True Positives} + \text{False Negatives}}$$

F1 Score:

The F1 score is the harmonic mean of precision and recall scores. A higher F1 score indicates a better quality classifier.

$$\text{F1 Score} = 2 * \frac{\text{Percision} * \text{Recall}}{\text{Percision} + \text{Recall}}$$

3.3.2 Performance comparison with other popular DNNs

When developing a deep learning model, it is essential to compare the model's performance with other popular deep learning models. The popular models have been extensively studied and widely used in various domains, setting a benchmark for performance evaluation. In this study, the proposed model is evaluated with the following well-known deep learning architecture: ResNet50, Vgg-16, MobileNet V3, and EfficientNet, by using the same dataset. Using the same dataset for the comparison of models allows a meaningful evaluation of performance metrics such as accuracy, recall, precision, and F1 score.

3.4 Model Deployment

After the training phase, the predictive deep-learning model was deployed using Flask, a powerful framework written in Python. The front end of the web application was developed using HTML and CSS, providing a user-friendly web interface that allows users to upload chest X-ray images for disease prediction. The Flask web application was developed and executed within a virtual environment to ensure proper isolation and dependency management. The virtual environment was created using the command line interface, the Command Prompt (CMD), by utilizing a tool named venv. The required dependencies including Flask, were installed using pip, the package manager for Python. A file named requirements.txt was included in the project directory along with the trained model and HTML files, which listed all the required packages and versions. The Flask application was run within the virtual environment in the CMD. This allowed the web application to be locally hosted and accessed, enabling users to interact with the application and perform chest X-ray classification.

CHAPTER 4

RESULTS

4. Results

4.1 Performance of the Proposed Model

The CNN model achieved promising results in predicting tuberculosis using chest X-rays. CNN achieved higher accuracy across all three classes: COVID-19, normal, and TB. The overall model accuracy was 98.34%, indicating the model's ability to classify chest X-ray images. **Table 4.1** shows the overall performance of the model. The class-specific accuracies were 99% for normal, 98% for TB, and 96% for COVID-19. Recall, precision, and F1 scores were also remarkable. The recall values were 0.99 for normal, 0.96 for COVID-19, and 0.98 for TB cases. The precision values were 0.98 for normal, 0.97 for COVID-19, and 0.98 for TB. The F1 scores were 0.99 for normal, 0.97 for COVID-19, and 0.98 for TB. These results highlight the high precision, recall, and f1-scores achieved across all classes, indicating the strong performance of the model in accurately classifying normal, COVID-19, and TB CXR images. **Table 4.2** represents the performance metrics including precision, recall and F1-Score for all three classes.

Table 4.1: Overall performance of the CNN Model

	Accuracy	Precision	Recall	F1-Score
CNN	0.98	0.98	0.98	0.98

Table 4.2: Accuracy, Precision, Recall and F1- Score of CNN Model for Each Class

Class	Accuracy	Precision	Recall	F1-Score
COVID-19	0.96	0.97	0.96	0.97
Normal	0.99	0.98	0.99	0.99
TB	0.98	0.98	0.98	0.98

To provide a visual representation of the model performance, **Figure 4.1** presents the confusion matrix of the proposed model. The true positives are represented by diagonal entries of the matrix, which are the CXR images that are correctly identified for each class. The misclassification of CXR images is represented by the off-diagonal entries, where rows correspond to the actual class label and columns to the predicted class. The training accuracy and the testing accuracy are shown in **Figure 4.2**, and the training and testing loss are shown in **Figure 4.3**. The x-axis represents the number of training iterations or epochs, and the y-axis represents the model accuracy. The training accuracy curve indicates an upward trend, demonstrating the models' ability to capture information from the training data; similarly, the upward testing accuracy curve indicates the model's ability to perform well on unseen data. The training and validation loss decrease and stabilize at a specific point, indicating that the model is an optimal fit, neither overfitting nor underfitting.

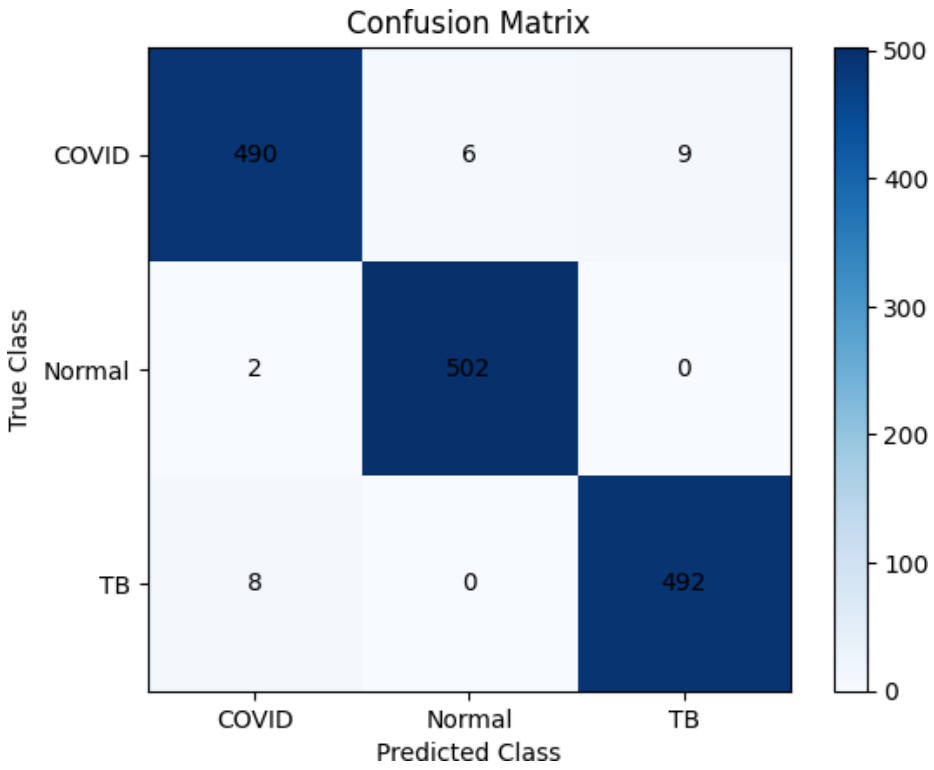

Figure 4.1: Confusion Matrix of the CNN Model

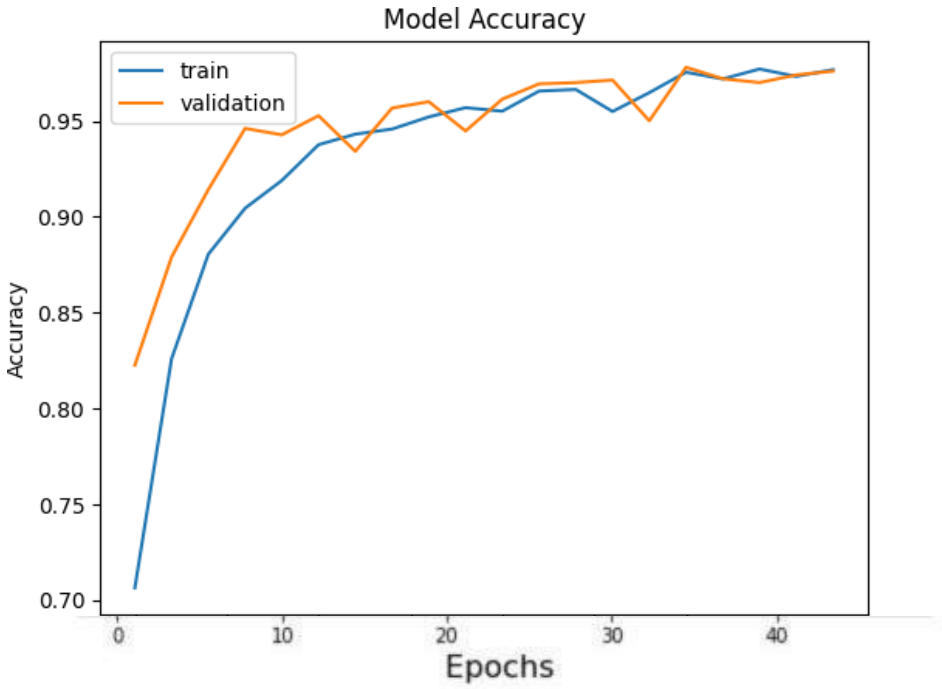

Figure 4.2: Training and Testing Accuracy against the Number of Epochs

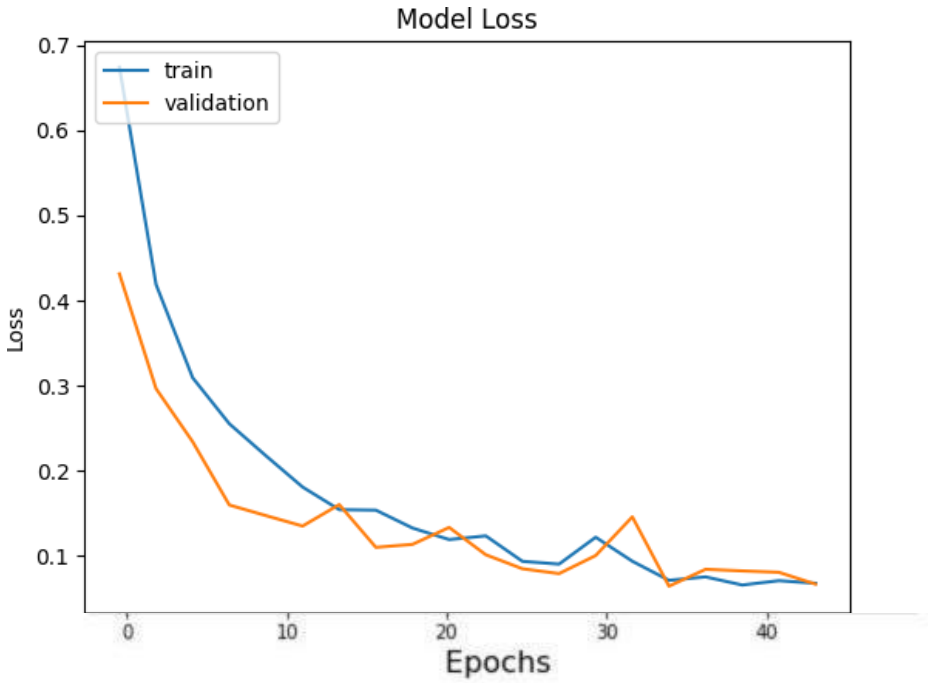

Figure 4.3: Training and Testing Loss against the Number of Epochs

4.2 Pre-trained Deep learning models

The pre-trained models VVG-16, Densenet-121, ResNet-50, and Inception-V3 were used to compare the performance of the CNN model, using the same dataset and evaluation matrices. Densenet-121 a pertained model consisting of 121 layers, achieved 0.9476 (94%) accuracy on training data and 0.9488 (94%) accuracy on testing data. The precision, recall and F1-score of the densenet-121 model were 0.95, 0.95, and 0.95 respectively; the same precision, recall and F1-score indicate that the model is performing consistently well in all classes. **Table 4.3** shows the performance metrics of densenet-121 for each class. In **Figure 4.4**, the confusion matrix illustrates the classification performance of the densenet-121 model on a test dataset comprising 500 TB, 504 normal and 505 COVID-19 chest X-ray images. Among the 500 TB images, the densenet-121 model correctly identified 463 images as TB, but misclassified 24 images as COVID-19 and 13 images as normal. For the COVID-19 test images, the model classified 474 images as COVID-19, while incorrectly labelling 22 images as normal and 9 images as TB. For normal test images, densenet-121 predicted 495 images as normal, but it misclassified the rest of the 9 images as COVID-19. The pre-trained model, ResNet50 achieved an accuracy of 0.86 (86%), precision of 0.88 (88%), recall of 0.86 (86%), and F1-Score of 0.86 (86%). The precision, recall and F1 score of the resnet-50 model for each class are shown in **Table 4.4** and **Figure 4.5** demonstrate the confusion matrix of resnet-50. Out of 500 TB test images, the resnet-50 correctly identified 427 images as TB, but it mistakenly classified 69 images as COVID-19 and 4 images as normal. Regarding the normal test images, the model accurately classified 402 images as normal, but it misclassified the 96 images as COVID-19 and 6 images as TB. Additionally for the COVID-19, the model correctly predicted 477 images as COVID-19, but it classified 10 images as normal and 20 images as TB. Inception-V3 achieved 0.93 (93%) accuracy, 0.94 precision, 0.93 recall and 0.9342 F1-score. The precision, recall and F1 score of the Inception-V3 model for each class are shown in **Table 4.5**. The confusion matrix presented in the **Figure 4.6** provides insights into the classification performance of Inception-V3. Among 500 TB images, the model correctly identified 412 images as TB. However, there was some misclassification, with 13 images as normal and 75 images of COVID-19. Turning to the COVID-19 test images, the Inceptio-V3 showed proficiency in identifying COVID-19 images; accurately classify 501 images out of 505 images and misclassified the remaining 4 images as normal. Moreover, the model classified 498 images as normal and the remaining 6 images as COVID-19 for the normal test images. The pre-trained

model VGG-16 achieved 0.96(96%) accuracy. The precision, recall and F1-score of the VGG-16 are 0.96, 0.95, and 0.95 respectively. The precision, recall and F1-Score of VGG-16 for each class are shown in **Table 4.6**. The classification performance of the VGG-16 model on test data is represented in **Figure 4.7**. Vgg-16 correctly identified 487 images as TB out of 500 TB test images, and mistakenly classified 3 images as normal and 10 images as COVID-19. For the normal class, the model classified 487 images as normal, 17 images as COVID-19 and 0 images as TB. Furthermore, the model classified 497 images as COVID-19, 9 images as normal and 1 image as TB for the COVID-19 test images. **Table 4.7** shows a performance comparison including accuracy, precision, recall and F1-Score of all models applied to the dataset used in this study. It is validated from the table that CNN obtained better performance in all performance metrics.

Table 4.3: Precision, Recall and F1- Score of Densenet-121 Model for Each Class

Class	Precision	Recall	F1-Score
COVID-19	0.93	0.94	0.94
Normal	0.93	0.98	0.96
TB	0.98	0.93	0.95

Table 4.4: Precision, Recall and F1- Score of Resnet-50 Model for Each Class

Class	Precision	Recall	F1-Score
COVID-19	0.74	0.94	0.83
Normal	0.97	0.80	0.87
TB	0.94	0.85	0.90

Table 4.5: Precision, Recall and F1- Score of Inception-V3 Model for Each Class

Class	Precision	Recall	F1-Score
COVID-19	0.98	0.99	0.98
Normal	0.97	0.99	0.98
TB	0.86	0.82	0.83

Table 4.6: Precision, Recall and F1- Score of VGG-16 Model for Each Class

Class	Precision	Recall	F1-Score
COVID19	0.94	0.97	0.95
Normal	0.97	0.96	0.96
TB	0.98	0.96	0.97

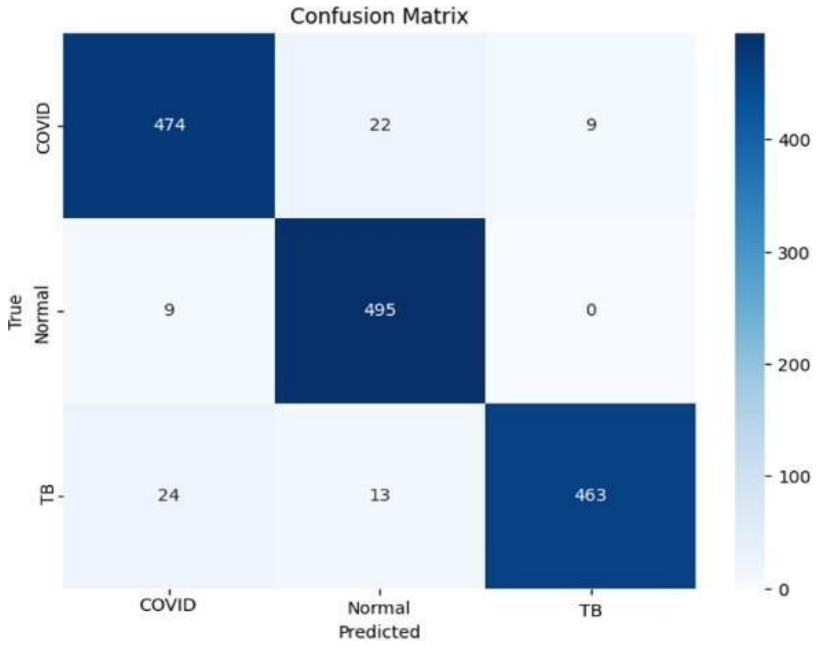

Figure 4.4: Confusion Matrix of the Densenet-121 Model

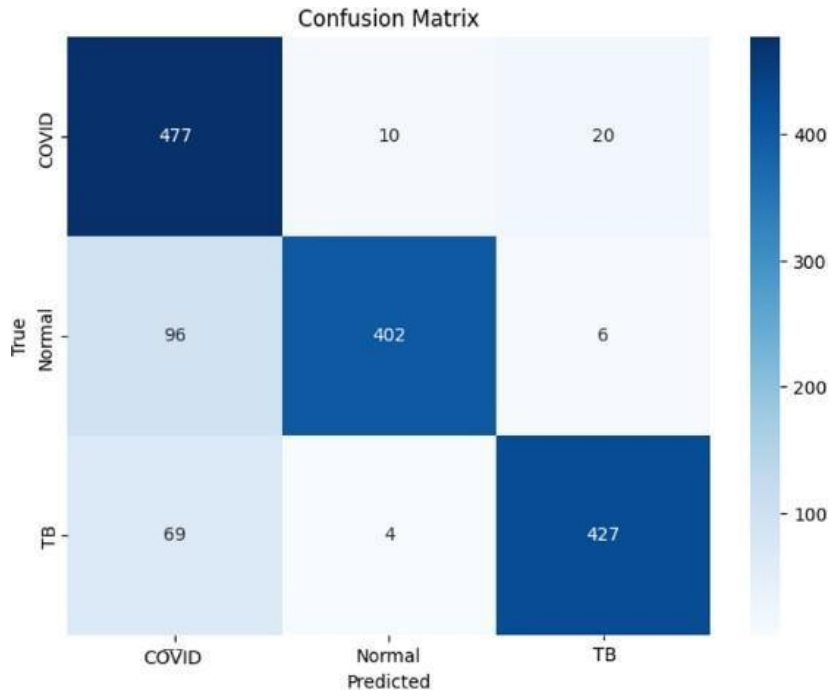

Figure 4.5: Confusion Matrix of Resnet-50 Model

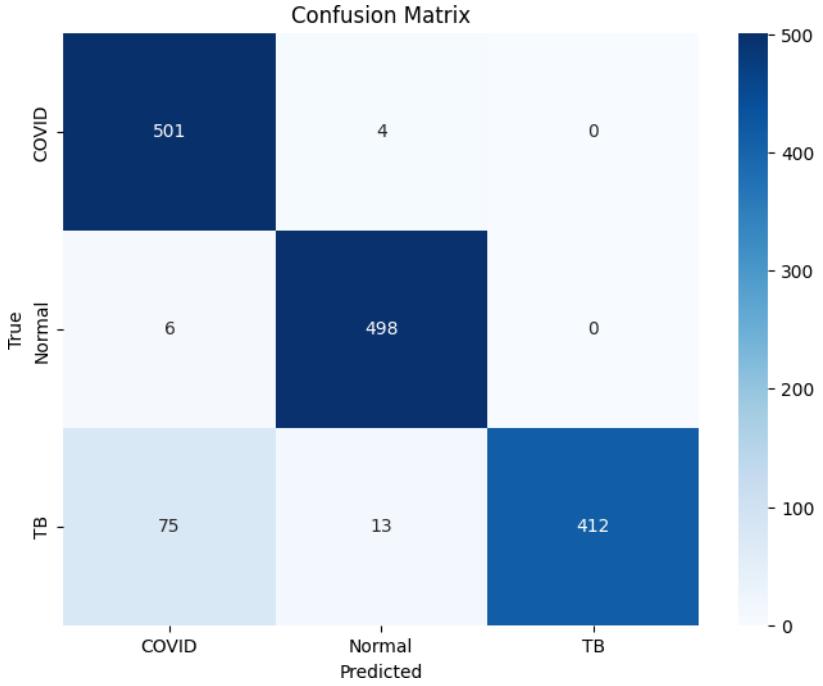

Figure 4.6: Confusion Matrix of Inception-V3 Model

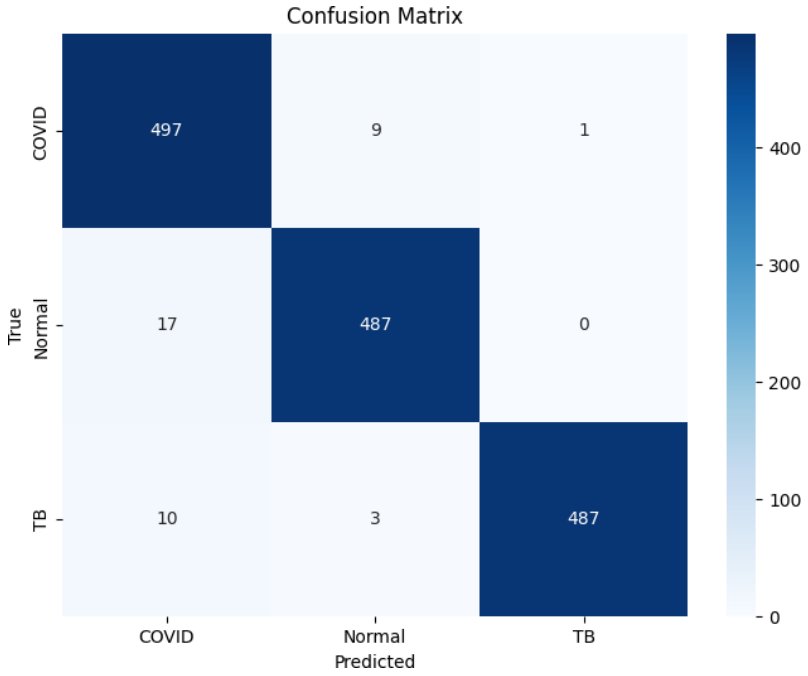

Figure 4.7: Confusion Matrix of VGG-16 Model

Table 4.7: Comparison of Accuracy, Precision, Recall and F1- Score of all the Models applied

Sr.	Model	Accuracy	Precision	Recall	F1-Score
1	CNN	0.97	0.98	0.98	0.98
2	DenseNet121	0.94	0.94	0.94	0.94
3	ResNet50	0.86	0.88	0.86	0.86
4	InceptionV3	0.93	0.94	0.93	0.93
5	VGG-16	0.96	0.96	0.95	0.95

4.3 Web Application

The deployed model for the classification of TB, COVID-19, and normal chest X-rays using Flask successfully provided accurate results. A user-friendly interface allows the users to upload the chest X-ray image for classification. **Figure 4.8** illustrates the user upload window where the users could upload their chest X-ray images. **Figure 4.9** shows the output window of the web application with the predicted label.

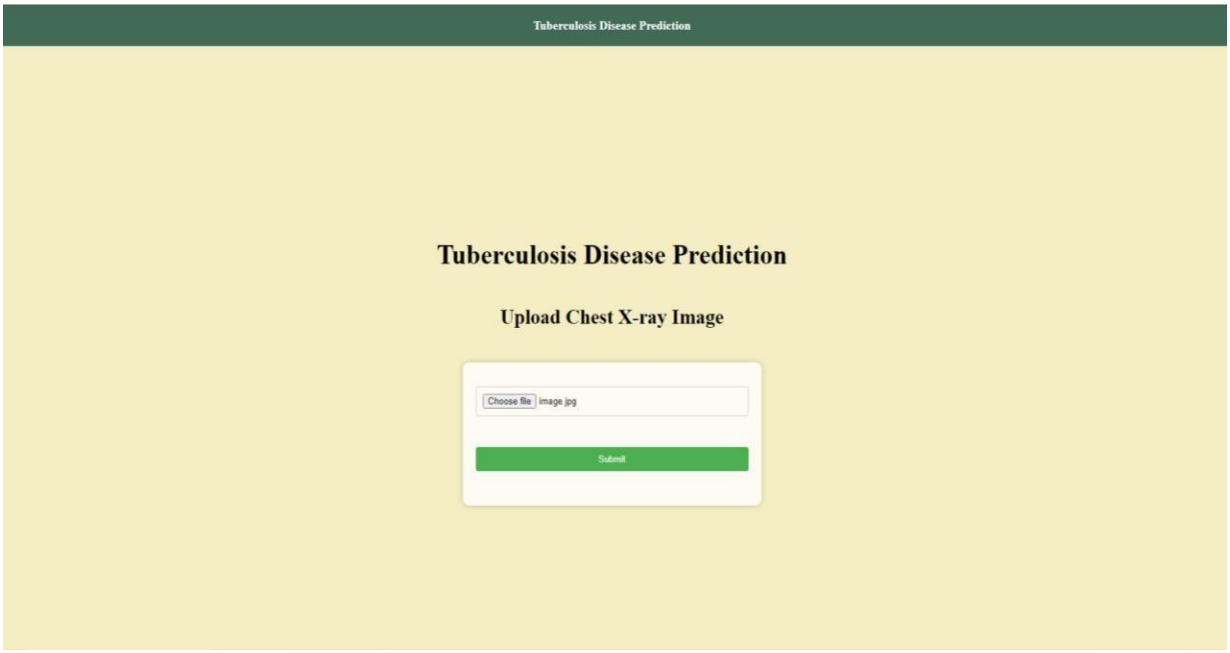

Figure 4.8: Upload Window for Chest X-ray Image

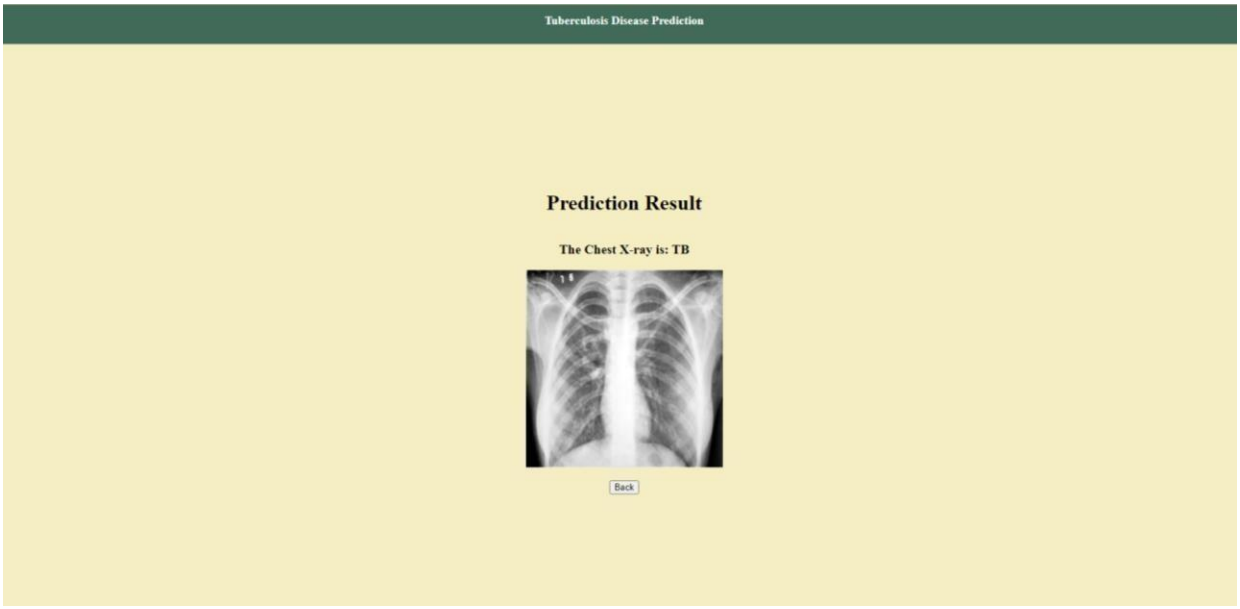

Figure 4.9: Output window with the predicted label

Discussion

In this proposed study, a deep learning-based model was developed to predict tuberculosis disease using chest X-ray images. The CNN model achieved an accuracy of 97%, sensitivity of 98%, precision of 98%, and recall of 98% in predicting tuberculosis disease from chest X-rays. Four popular pre-trained models, namely VGG-16, Densenet-121, Resnet-50, and Inception-v3 were also used for the performance comparison. VGG-16, Resnet-50, Densenet-121, and Inception-v3 achieved an accuracy of 96%, 86%, 94%, and 93% respectively. For our dataset, CNN achieved higher accuracy among all applied models. Table 4.7 outlines the performance matrices of all the models applied to the dataset. The achieved accuracy of the proposed model indicates its effectiveness in differentiating tuberculosis, COVID-19, and normal chest X-rays. The high accuracy of the model in the classification of tuberculosis demonstrates that the model has learned meaningful features and patterns necessary for the detection of TB from the chest X-ray dataset. Moreover, a balanced dataset consisting of 2500 TB, 2517 normal, and 2534 COVID-19 chest X-rays were utilized. By using a balanced dataset, this study addressed the issue of class imbalance, which has been a challenge in some previous studies[77] [79]. In addition to achieving good results in terms of accuracy, sensitivity, precision, recall, and addressing class imbalance issues, the proposed model was deployed into a web application using the Flask framework. The web application offers a user-friendly interface where users can input the chest X-ray image and get the model's prediction in the output window. This can also help the healthcare professional to make a decision about TB disease and assist in quick and early diagnosis based on chest X-rays. The proposed model may be integrated into mobile apps, and healthcare professionals and interested users access the diagnostic model directly from their smartphones.

Conclusion

Conclusion

In conclusion, this study demonstrates the effectiveness of deep learning approaches in medical imaging to diagnose pulmonary diseases. The proposed model is not only confined to TB verse normal, but it also predicts COVID-19. The high accuracy achieved by the model indicates its ability to predict the disease from chest X-rays accurately. Addressing the issue of TB misclassification to other pulmonary diseases, the proposed model achieved good results in accurately predicting TB disease from chest x-rays and aiding in the timely treatment and control of the disease. Furthermore, successfully deploying the model as a user-friendly web application provides healthcare professionals with a reliable tool for classifying tuberculosis disease. In the future, expanding the dataset to add more data from diverse regions of Pakistan and incorporating more pulmonary diseases such as pneumonia can significantly increase the classification capabilities of the model.

REFERENCES

REFERENCES

References

[1] S. V. Patil, S. Toshniwal, G. Gondhali, and D. Patil, "Pulmonary tuberculosis with cardiac dysfunction: An ignored combination!," *Electron. J. Gen. Med.*, vol. 20, no. 1, pp. 1–5, 2023, doi: 10.29333/ejgm/12679.

[2] A. R. Analysis, O. F. The, T. Schedule, and O. F. Pulmonary, "A retrospective analysis of the co-morbidities and treatment schedule of pulmonary tuberculosis reporting at ananta institute of medical sciences," vol. 12, no. 7, pp. 1193–1215, 2023, doi: 10.20959/wjpr20237-28069.

[3] A. Aggarwal *et al.*, "Clinical & immunological erythematosus patients characteristics in systemic lupus Maryam," *J. Dent. Educ.*, vol. 76, no. 11, pp. 1532–9, 2012, doi: 10.4103/ijmr.IJMR.

[4] M. S. Goudiaby, L. D. Gning, M. L. Diagne, B. M. Dia, H. Rwezaura, and J. M. Tchuenche, "Optimal control analysis of a COVID-19 and tuberculosis co-dynamics model," *Informatics Med. Unlocked*, vol. 28, p. 100849, 2022, doi: 10.1016/j.imu.2022.100849.

[5] S. Taufiq, M. Waqar, M. N. Sharif, and S. R. Abbas, "Towards portable rapid TB biosensor: Detecting Mycobacterium tuberculosis in raw sputum samples using functionalized screen printed electrodes," *Bioelectrochemistry*, vol. 150, no. December 2022, p. 108353, 2023, doi: 10.1016/j.bioelechem.2022.108353.

[6] M. S. Islam *et al.*, "Examining pulmonary TB patient management and healthcare workers exposures in two public tertiary care hospitals, Bangladesh," *PLOS Glob. Public Heal.*, vol. 2, no. 1, p. e0000064, 2022, doi: 10.1371/journal.pgph.0000064.

[7] H. K. Mohajan, "Munich Personal RePEc Archive Tuberculosis is a Fatal Disease among Some Developing Countries of the World," *Am. J. Infect. Dis. Microbiol.*, vol. 3, no. 1, pp. 18–31, 2015.

[8] A. S. Rao, S. Shamitha, S. R. G. Tarun, S. U. Priya, and V. R. B. Prasad, "A Survey on Diagnosing Pulmonary Diseases," *2023 IEEE Int. Students' Conf. Electr. Electron. Comput. Sci. SCEECS 2023*, pp. 1–5, 2023, doi: 10.1109/SCEECS57921.2023.10063115.

[9] C. Report and D. C. Report, "Annals of Clinical Case Reports Miliary Nodules Caused by

REFERENCES

Multi Drug Resistant Mycobacterium tuberculosis - Rare Presentation of Common," vol. 7, no. Figure 1, pp. 7–9, 2022.

[10] "The potential impact of novel tuberculosis vaccine introduction on economic growth in low- and middle-income countries Authors," vol. 1, no. 617, pp. 1–28, 2022.

[11] M. Milaham *et al.*, "Assessment of tuberculosis case notification rate: spatial mapping of hotspot, coverage and diagnostics in Katsina State, north-western Nigeria," *J. Public Health Africa*, vol. 13, no. 3, 2022, doi: 10.4081/jphia.2022.2040.

[12] T. Akpobolokemi, R. T. Martinez-Nunez, and B. T. Raimi-Abraham, "Tackling the global impact of substandard and falsified and unregistered/unlicensed anti-tuberculosis medicines," *J. Med. Access*, vol. 6, p. 239920262110704, 2022, doi: 10.1177/23992026211070406.

[13] J. P. Zellweger, G. Sotgiu, M. Corradi, and P. Durando, "The diagnosis of latent tuberculosis infection (Ltbi): Currently available tests, future developments, and perspectives to eliminate tuberculosis (tb)," *Med. del Lav.*, vol. 111, no. 3, pp. 170–183, 2020, doi: 10.23749/mdl.v111i3.9983.

[14] P. F. Rebeiro *et al.*, "Knowledge and stigma of latent tuberculosis infection in Brazil: Implications for tuberculosis prevention strategies," *BMC Public Health*, vol. 20, no. 1, pp. 1–10, 2020, doi: 10.1186/s12889-020-09053-1.

[15] M. A. Behr, E. Kaufmann, J. Duffin, P. H. Edelstein, and L. Ramakrishnan, "Latent tuberculosis: Two centuries of confusion," *Am. J. Respir. Crit. Care Med.*, vol. 204, no. 2, pp. 142–148, 2021, doi: 10.1164/rccm.202011-4239PP.

[16] C. A. Peloquin and G. R. Davies, "The Treatment of Tuberculosis," *Clin. Pharmacol. Ther.*, vol. 110, no. 6, pp. 1455–1466, 2021, doi: 10.1002/cpt.2261.

[17] J. Ahmad *et al.*, "Demographics and Critical Analysis of Smear-Positive Tuberculosis in District Abbottabad, Pakistan: Implementations for Future Challenges," *Pak-Euro J. Med. Life Sci.*, vol. 4, no. 4, pp. 319–326, 2021, doi: 10.31580/pjmls.v4i4.2164.

[18] Z. J. Madewell, Y. Yang, I. M. L. Jr, M. E. Halloran, and N. E. Dean, "Active or latent tuberculosis increases susceptibility to COVID-19 and disease severity," *medRxiv*, no. 165,

pp. 1–13, 2020.

[19] A. Sharma *et al.*, "An accurate artificial intelligence system for the detection of pulmonary and extra pulmonary Tuberculosis," *Tuberculosis*, vol. 131, no. November, p. 102143, 2021, doi: 10.1016/j.tube.2021.102143.

[20] R. Gopalaswamy, V. N. A. Dusthackeer, S. Kannayan, and S. Subbian, "Extrapulmonary Tuberculosis—An Update on the Diagnosis, Treatment and Drug Resistance," *J. Respir.*, vol. 1, no. 2, pp. 141–164, 2021, doi: 10.3390/jor1020015.

[21] G. R. Kathamuthu *et al.*, "Matrix Metalloproteinases and Tissue Inhibitors of Metalloproteinases Are Potential Biomarkers of Pulmonary and Extra-Pulmonary Tuberculosis," *Front. Immunol.*, vol. 11, no. March, pp. 1–13, 2020, doi: 10.3389/fimmu.2020.00419.

[22] S. A. Ohene, M. I. Bakker, J. Ojo, A. Toonstra, D. Awudi, and P. Klatser, "Extra-pulmonary tuberculosis: A retrospective study of patients in Accra, Ghana," *PLoS One*, vol. 14, no. 1, pp. 1–13, 2019, doi: 10.1371/journal.pone.0209650.

[23] K. S. Gunasekera *et al.*, "Diagnostic Challenges in Childhood Pulmonary Tuberculosis—Optimizing the Clinical Approach," *Pathogens*, vol. 11, no. 4, pp. 1–11, 2022, doi: 10.3390/pathogens11040382.

[24] A. S. Richards *et al.*, "Articles Quantifying progression and regression across the spectrum of pulmonary tuberculosis : a data synthesis study," pp. 684–692, doi: 10.1016/S2214-109X(23)00082-7.

[25] A. Pooran, E. Pieterson, M. Davids, G. Theron, and K. Dheda, "What is the Cost of Diagnosis and Management of Drug Resistant Tuberculosis in South Africa?," *PLoS One*, vol. 8, no. 1, 2013, doi: 10.1371/journal.pone.0054587.

[26] G. Abate, H. Miörner, O. Ahmed, and S. E. Hoffner, "Drug resistance in Mycobacterium tuberculosis strains isolated from re- treatment cases of pulmonary tuberculosis in Ethiopia: Susceptibility to first-line and alternative drugs," *Int. J. Tuberc. Lung Dis.*, vol. 2, no. 7, pp. 580–584, 1998.

[27] K. Dheda, H. Cox, A. Esmail, S. Wasserman, K. C. Chang, and C. Lange, "Recent

controversies about MDR and XDR-TB: Global implementation of the WHO shorter MDR-TB regimen and bedaquiline for all with MDR-TB?," *Respirology*, vol. 23, no. 1, pp. 36–45, 2018, doi: 10.1111/resp.13143.

[28] P. E. Alexander and P. De, "The emergence of extensively drug-resistant tuberculosis (TB): TB/HIV coinfection, multidrug-resistant TB and the resulting public health threat from extensively drug-resistant TB, globally and in Canada," *Can. J. Infect. Dis. Med. Microbiol.*, vol. 18, no. 5, pp. 289–291, 2007, doi: 10.1155/2007/986794.

[29] G. B. Migliori *et al.*, "Review of multidrug-resistant and extensively drug-resistant TB: Global perspectives with a focus on sub-Saharan Africa," *Trop. Med. Int. Heal.*, vol. 15, no. 9, pp. 1052–1066, 2010, doi: 10.1111/j.1365-3156.2010.02581.x.

[30] P. Singh, S. Kant, P. Gaur, A. Tripathi, and S. Pandey, "Extra Pulmonary Tuberculosis: An Overview and Review of Literature," *Int. J. Life-Sciences Sci. Res.*, vol. 4, no. 1, pp. 2016–2018, 2018, doi: 10.21276/ijlssr.2018.4.1.5.

[31] A. Cherian and T. Sv, "Central nervous system tuberculosis," vol. 11, no. 1, 2011.

[32] A. N.-A. M Ramirez-Lapausa, A Menendez-Saldana, "Extrapulmonary tuberculosis: An overview," *Am. Fam. Physician*, vol. 72, no. 9, pp. 1761–1768, 2005, doi: 10.5772/intechopen.81322.

[33] J. Y. Lee, "Diagnosis and treatment of extrapulmonary tuberculosis," *Tuberc. Respir. Dis. (Seoul).*, vol. 78, no. 2, pp. 47–55, 2015, doi: 10.4046/trd.2015.78.2.47.

[34] S. G. Mortazavi-Moghaddam, A. S. Pagheh, E. Ahmadpour, A. Barac, and A. Ebrahimzadeh, "Tuberculous meningitis and miliary tuberculosis in Iran: A review," *Asian Pac. J. Trop. Med.*, vol. 15, no. 4, pp. 143–152, 2022, doi: 10.4103/1995-7645.343880.

[35] K. Singh, S. Hyatali, S. Giddings, K. Singh, and N. Bhagwandass, "Corrigendum to 'Miliary Tuberculosis Presenting with ARDS and Shock: A Case Report and Challenges in Current Management and Diagnosis,'" *Case Reports Crit. Care*, vol. 2018, pp. 1–1, 2018, doi: 10.1155/2018/2073618.

[36] S. K. Sharma, A. Mohan, and A. Sharma, "Miliary tuberculosis: A new look at an old foe," *J. Clin. Tuberc. Other Mycobact. Dis.*, vol. 3, pp. 13–27, 2016, doi:

10.1016/j.jctube.2016.03.003.

[37] F. Vanhoenacker, D. Sanghvi, and A. De Backer, "Imaging features of extraaxial musculoskeletal tuberculosis," *Indian J. Radiol. Imaging*, vol. 19, no. 3, pp. 176–186, 2009, doi: 10.4103/0971-3026.54873.

[38] V. Agrawal, P. R. Patgaonkar, and S. P. Nagariya, "Tuberculosis of spine," *J. Craniovertebr. Junction Spine*, vol. 1, no. 2, pp. 74–85, 2010, doi: 10.4103/0974-8237.77671.

[39] T. Zajaczkowski, "Genitourinary tuberculosis: Historical and basic science review: Past and present," *Cent. Eur. J. Urol.*, vol. 65, no. 4, pp. 182–187, 2012, doi: 10.5173/ceju.2012.04.art1.

[40] S. Y. Rodriguez-Takeuchi, M. E. Renjifo, and F. J. Medina, "Extrapulmonary tuberculosis: Pathophysiology and imaging findings," *Radiographics*, vol. 39, no. 7, pp. 2023–2037, 2019, doi: 10.1148/rg.2019190109.

[41] N. Mandal, P. K. Anand, S. Gautam, S. Das, and T. Hussain, "Diagnosis and treatment of paediatric tuberculosis: An insight review," *Crit. Rev. Microbiol.*, vol. 43, no. 4, pp. 466–480, 2017, doi: 10.1080/1040841X.2016.1262813.

[42] C. C. Boehme *et al.*, "Feasibility, diagnostic accuracy, and effectiveness of decentralised use of the Xpert MTB/RIF test for diagnosis of tuberculosis and multidrug resistance: A multicentre implementation study," *Lancet*, vol. 377, no. 9776, pp. 1495–1505, 2011, doi: 10.1016/S0140-6736(11)60438-8.

[43] M. P. Sekadde *et al.*, "Evaluation of the Xpert MTB/RIF test for the diagnosis of childhood pulmonary tuberculosis in Uganda: A cross-sectional diagnostic study," *BMC Infect. Dis.*, vol. 13, no. 1, 2013, doi: 10.1186/1471-2334-13-133.

[44] S. M. Arend *et al.*, "Comparison of two interferon-γ assays and tuberculin skin test for tracing tuberculosis contacts," *Am. J. Respir. Crit. Care Med.*, vol. 175, no. 6, pp. 618–627, 2007, doi: 10.1164/rccm.200608-1099OC.

[45] Y. Hamada *et al.*, "Predictive performance of interferon-gamma release assays and the tuberculin skin test for incident tuberculosis: an individual participant data meta-analysis,"

eClinicalMedicine, vol. 56, p. 101815, 2023, doi: 10.1016/j.eclinm.2022.101815.

[46] G. Ferrara *et al.*, "Use in routine clinical practice of two commercial blood tests for diagnosis of infection with Mycobacterium tuberculosis: a prospective study," *Lancet*, vol. 367, no. 9519, pp. 1328–1334, 2006, doi: 10.1016/S0140-6736(06)68579-6.

[47] F. P. A. Van Deun, "Limitations and requirements for quality control of sputum smear microscopy for acid-fast bacilli."

[48] N. T. Q. Nhu *et al.*, "Evaluation of genexpert MTB/RIF for diagnosis of tuberculous meningitis," *J. Clin. Microbiol.*, vol. 52, no. 1, pp. 226–233, 2014, doi: 10.1128/JCM.01834-13.

[49] J. Donovan *et al.*, "Xpert MTB/RIF Ultra versus Xpert MTB/RIF for the diagnosis of tuberculous meningitis: a prospective, randomised, diagnostic accuracy study," *Lancet Infect. Dis.*, vol. 20, no. 3, pp. 299–307, 2020, doi: 10.1016/S1473-3099(19)30649-8.

[50] Z. Z. Qin *et al.*, "Tuberculosis detection from chest x-rays for triaging in a high tuberculosis-burden setting: an evaluation of five artificial intelligence algorithms," *Lancet Digit. Heal.*, vol. 3, no. 9, pp. e543–e554, 2021, doi: 10.1016/S2589-7500(21)00116-3.

[51] C. Dasanayaka and M. B. Dissanayake, "Deep Learning Methods for Screening Pulmonary Tuberculosis Using Chest X-rays," *Comput. Methods Biomech. Biomed. Eng. Imaging Vis.*, vol. 9, no. 1, pp. 39–49, 2021, doi: 10.1080/21681163.2020.1808532.

[52] H. Malik, T. Anees, M. Din, and A. Naeem, "CDC_Net: multi-classification convolutional neural network model for detection of COVID-19, pneumothorax, pneumonia, lung Cancer, and tuberculosis using chest X-rays," *Multimed. Tools Appl.*, pp. 13855–13880, 2022, doi: 10.1007/s11042-022-13843-7.

[53] T. B. Chandra, K. Verma, B. K. Singh, D. Jain, and S. S. Netam, "Automatic detection of tuberculosis related abnormalities in Chest X-ray images using hierarchical feature extraction scheme," *Expert Syst. Appl.*, vol. 158, p. 113514, 2020, doi: 10.1016/j.eswa.2020.113514.

[54] A. Bhargava and H. D. Shewade, "The potential impact of the COVID-19 response related lockdown on TB incidence and mortality in India," *Indian J. Tuberc.*, vol. 67, no. 4, pp.

S139–S146, 2020, doi: 10.1016/j.ijtb.2020.07.004.

[55] S. Razzaq, A. Zahidie, and Z. Fatmi, "Estimating the pre- and post-diagnosis costs of tuberculosis for adults in Pakistan: household economic impact and costs mitigating strategies," *Glob. Heal. Res. Policy*, vol. 7, no. 1, 2022, doi: 10.1186/s41256-022-00259-x.

[56] Common Lab Tests in Pakistan, "Tuberculosis testing in Pakistan."

[57] K. C. C. Keertan Dheda, Tahlia Perumal, Harry Moultrie, Rubeshan Perumal, Aliasgar Esmail, Alex J Scott, Zarir Udwadia, E. K. Jonathan Peter, Anil Pooran, Arne von Delft, Dalene von Delft, Neil Martinson, Marian Loveday, Salome Charalambous, and M. P. Waasila Jassat, Cheryl Cohen, Stefano Tempia, Kevin Fennelly, "The intersecting pandemics of tuberculosis and COVID-19: population-level and patient-level impact, clinical presentation, and corrective interventions," no. January, pp. 19–21, 2020.

[58] M. Cellina, M. Orsi, T. Toluian, C. V. Pittino, and G. Oliva, "False negative chest X-Rays in patients affected by COVID-19 pneumonia and corresponding chest CT findings," no. January, 2020.

[59] A. E. H. Ahmed, A. S. Ibrahim, and S. M. Elshafie, "Pulmonary hypertension in patients with treated pulmonary tuberculosis: Analysis of 14 consecutive cases," *Clin. Med. Insights Circ. Respir. Pulm. Med.*, vol. 5, no. 1, pp. 1–5, 2011, doi: 10.4137/CCRPM.S6437.

[60] T. Afum *et al.*, "Diagnosis of tuberculosis among COVID-19 suspected cases in Ghana," *PLoS One*, vol. 16, no. 12 December, pp. 1–8, 2021, doi: 10.1371/journal.pone.0261849.

[61] N. A. GABRIELLE GERBINO, "MISSED TB DIAGNOSIS DURING THE COVID-19 PANDEMIC: MYTH OR REAL," no. January, 2020.

[62] M. Wei, Y. Zhao, Z. Qian, B. Yang, J. Xi, and J. Wei, "Pneumonia caused by Mycobacterium tuberculosis Meili," no. January, 2020.

[63] Rajesh, T. Babu, R. R. Nair, and P. Pechetti, "Detection of Tuberculosis using a Multi-model Classification Approach on CXR Images," *2022 Int. Conf. Artif. Intell. Data Eng.*, pp. 252–258, 2023, doi: 10.1109/aide57180.2022.10060675.

[64] J. Devasia, H. Goswami, S. Lakshminarayanan, M. Rajaram, and S. Adithan, "Deep

learning classification of active tuberculosis lung zones wise manifestations using chest X-rays: a multi label approach," *Sci. Rep.*, vol. 13, no. 1, pp. 1–15, 2023, doi: 10.1038/s41598-023-28079-0.

[65] H. Latifi-Pupovci, M. Selmonaj, B. Ahmetaj-Shala, M. Dushi, and V. Grajqevci, "Incidence of haematological malignancies in Kosovo—A post 'uranium war' concern," *PLoS One*, vol. 15, no. 5, pp. 1–13, 2020, doi: 10.1371/journal.pone.0232063.

[66] M. R. A. van Cleeff, L. E. Kivihya-Ndugga, H. Meme, J. A. Odhiambo, and P. R. Klatser, "The role and performance of chest X-ray for the diagnosis of tuberculosis: A cost-effective analysis in Nairobi, Kenya," *BMC Infect. Dis.*, vol. 5, pp. 1–9, 2005, doi: 10.1186/1471-2334-5-111.

[67] P. Clowes, F. Mhimbira, S. Mfinanga, A. Rachow, K. Reither, and M. Hoelscher, "Screening for pulmonary tuberculosis in a Tanzanian prison and computer-aided interpretation of chest X-rays," *World Heal. Organ. Reg. Publ. - Eur. Ser.*, vol. I, no. 56, pp. 31–49, 1995.

[68] Z. A. Ahmed Iqbal, Muhammad Usman, "Tuberculosis chest X-ray detection using CNN-based hybrid segmentation and classification approach, Biomedical Signal Processing and Control," vol. 84, no. 1746–8094, 2023, [Online]. Available: https://doi.org/10.1016/j.bspc.2023.104667

[69] G. M. M. Alshmrani, Q. Ni, R. Jiang, H. Pervaiz, and N. M. Elshennawy, "A deep learning architecture for multi-class lung diseases classification using chest X-ray (CXR) images," *Alexandria Eng. J.*, vol. 64, pp. 923–935, 2023, doi: 10.1016/j.aej.2022.10.053.

[70] F. Mancini, N. Bolognini, P. Haggard, and G. Vallar, "Computer-aided Detection of Tuberculosis from Microbiological and Radiographic Images," *Nat. Publ. Gr.*, no. January, pp. 1–9, 2012, doi: 10.1162/dint.

[71] Z. Naz, M. U. G. Khan, T. Saba, A. Rehman, H. Nobanee, and S. A. Bahaj, "An Explainable AI-Enabled Framework for Interpreting Pulmonary Diseases from Chest Radiographs," *Cancers (Basel).*, vol. 15, no. 1, 2023, doi: 10.3390/cancers15010314.

[72] M. Constantinou, T. Exarchos, A. G. Vrahatis, and P. Vlamos, "COVID-19 Classification

on Chest X-ray Images Using Deep Learning Methods," *Int. J. Environ. Res. Public Health*, vol. 20, no. 3, 2023, doi: 10.3390/ijerph20032035.

[73] M. Bhandari, T. B. Shahi, B. Siku, and A. Neupane, "Explanatory classification of CXR images into COVID-19, Pneumonia and Tuberculosis using deep learning and XAI," *Comput. Biol. Med.*, vol. 150, no. September, p. 106156, 2022, doi: 10.1016/j.compbiomed.2022.106156.

[74] V. Ravi, V. Acharya, and M. Alazab, "A multichannel EfficientNet deep learning-based stacking ensemble approach for lung disease detection using chest X-ray images," *Cluster Comput.*, vol. 26, no. 2, pp. 1181–1203, 2022, doi: 10.1007/s10586-022-03664-6.

[75] J. N. S. & A. D. D. Ketki C. Pathak, Swathi S. Kundaram, "Diagnosis and Analysis of Tuberculosis Disease Using Simple Neural Network and Deep Learning Approach for Chest X-Ray Images," *Springer, Cham*, 2022, [Online]. Available: https://doi.org/10.1007/978-3-030-76732-7_4

[76] C. J. Liu *et al.*, "A deep learning model using chest X-ray for identifying TB and NTM-LD patients: a cross-sectional study," *Insights Imaging*, vol. 14, no. 1, 2023, doi: 10.1186/s13244-023-01395-9.

[77] V. T. Q. Huy and C. M. Lin, "An Improved Densenet Deep Neural Network Model for Tuberculosis Detection Using Chest X-Ray Images," *IEEE Access*, vol. 11, no. April, pp. 42839–42849, 2023, doi: 10.1109/ACCESS.2023.3270774.

[78] G. Simi Margarat *et al.*, "Early Diagnosis of Tuberculosis Using Deep Learning Approach for IOT Based Healthcare Applications," *Comput. Intell. Neurosci.*, vol. 2022, 2022, doi: 10.1155/2022/3357508.

[79] S. M. Fati, E. M. Senan, and N. ElHakim, "Deep and Hybrid Learning Technique for Early Detection of Tuberculosis Based on X-ray Images Using Feature Fusion," *Appl. Sci.*, vol. 12, no. 14, 2022, doi: 10.3390/app12147092.

[80] R. Antony, J. Davies, and R. S. Kumar, "A Review on Tuberculosis Identification Using Convolutional Neural Networks," *8th Int. Conf. Adv. Comput. Commun. Syst. ICACCS 2022*, vol. 1, pp. 1365–1368, 2022, doi: 10.1109/ICACCS54159.2022.9785041.

REFERENCES

[81] A. U. Ibrahim, F. Al-Turjman, M. Ozsoz, and S. Serte, "No Title," *Biomed. Eng. / Biomed. Tech.*, vol. 67, no. 6, pp. 513–524, 2022, doi: doi:10.1515/bmt-2021-0310.

[82] P. Geetha Pavani, B. Biswal, M. V. S. Sairam, and N. Bala Subrahmanyam, "A semantic contour based segmentation of lungs from chest x-rays for the classification of tuberculosis using Naïve Bayes classifier," *Int. J. Imaging Syst. Technol.*, vol. 31, no. 4, pp. 2189–2203, 2021, doi: 10.1002/ima.22556.

[83] M. Ayaz, F. Shaukat, and G. Raja, "Ensemble learning based automatic detection of tuberculosis in chest X-ray images using hybrid feature descriptors," *Phys. Eng. Sci. Med.*, vol. 44, no. 1, pp. 183–194, 2021, doi: 10.1007/s13246-020-00966-0.

[84] S. Vajda *et al.*, "Feature Selection for Automatic Tuberculosis Screening in Frontal Chest Radiographs," *J. Med. Syst.*, vol. 42, no. 8, 2018, doi: 10.1007/s10916-018-0991-9.

[85] "COVID19 with Pneumonia and Normal Chest Xray(PA) Dataset." https://www.kaggle.com/datasets/amanullahasraf/covid19-pneumonia-normal-chest-xray-pa-dataset

[86] "COVID-19 Chest X-ray images and Lung masks Database", [Online]. Available: https://www.kaggle.com/code/cdaman/covid-19-chest-xray-with-gradcam/input